Arafeh. Reem B. <u>Strategy to Design a Stratified Lamellar Corneal Stroma Construct</u>. Masters of Science (Biomedical Sciences), July 2nd, 2008, 103pp., 1 table, 42 illustrations, bibliography, 63 titles.

Cornea is the transparent portion of the eye. Its three cellular compartments: the epithelium, stroma, and endothelium, are optimized for transparency and focusing. Although corneal grafting with donor corneas is a successful treatment to restore vision, there is an acute shortage of appropriate quality donor tissue. Tissue engineering is a new approach that addresses this shortage.

In this thesis it was demonstrated that lamellar stromal structure is reproduced by stacking thin collagen films. Collagen fibril organization in the thin films directs cellular alignment allowing assembly of an orthogonal stroma construct that transmits more light than most other published constructs and is optically active. Whereas the cell alignment and lamellar arrangement were successful, optimization of optical properties is a major future goal.

STRATEGY TO DESIGN A STRATIFIED LAMELLAR CORNEAL STROMA CONSTRUCT
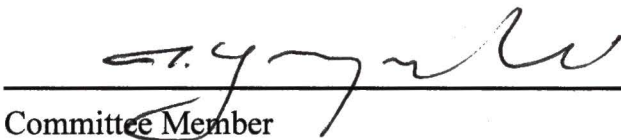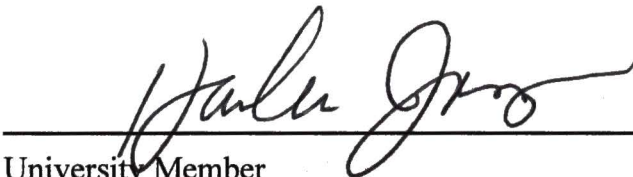
Reem B. Arafeh, B.S.
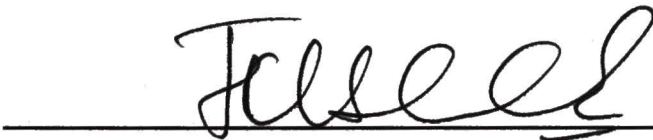
APPROVED:

_____

Major Professor
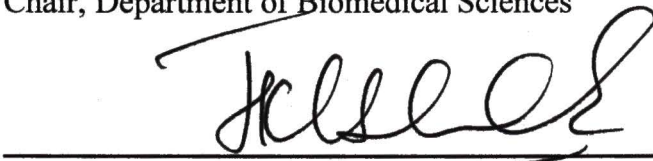
_____

Committee Member

_____

Committee Member

_____

University Member

_____

Chair, Department of Biomedical Sciences

_____

Dean, Graduate School of Biomedical Sciences

STRATEGY TO DESIGN A STRATIFIED LAMELLAR CORNEAL STROMA

CONSTRUCT

THESIS

Presented to the Graduate Council of the

Graduate School of Biomedical Sciences

University of North Texas

Health Science Center at Fort Worth

In Partial Fulfillment of the Requirements

For the Degree of

MASTER OF SCIENCE

By

Reem B. Arafeh, B.S.

Fort Worth, Texas

July 2008

ACKNOWLEDGEMENTS

I would like to thank everybody who contributed to the completion of this master's thesis project. This project would not have been possible without the guidance, perseverance, and support of my major advisor, Dr. Dan Dimitrijevich, who pushed me everyday to do better and think "outside the box". I would like to thank all my committee members; Dr. Ignacy Gryczynski, Dr. Harlan Jones, and Dr. Raghu Krishnamoorthy, who supported my project and believed in my ideas. I can not attribute the success of this project without acknowledging my lab mates; Jwalitha Shankardas, Anupam Sule, and Tasneem Putliwala. In the lab we work as a team, and it is our combined efforts in a cooperative environment that keeps our projects progressing and developing the way they have.

I would also like to thank I-fen Chang for training me to operate the confocal microscope, Anne-Marie Zinkernagel for helping me with the paraffin cross-sections, and the entire Gryczynski lab for all their help and advice in the molecular fluorescence aspect of this project.

Finally, I am forever indebted to my parents; Samar and Bassel and my brother Rashad for their understanding, endless patience, support and encouragement when it was most required. Thank you!

TABLE OF CONTENTS

LIST OF TABLES

CHAPTER I

LIST OF ILLUSTRATIONS

CHAPTER I

CHAPTER II

CHAPTER III

CHAPTER V

CHAPTER I

INTRODUCTION

Anatomy and Physiology of the Cornea

The cornea is a very organized and complex avascular tissue that is located at the anterior segment of the eye. It maintains visual acuity and is a major contributor of the eye's optical properties. It serves as a living optical lens with curvature that provides focusing power, and over 50% of its lamellar composition protects the inner eye structures from penetrating injuries; it also supports the tear film and prevents microbes and pathogens from entering the eye [1, 2]. Its complexity and uniqueness is due to the fact that it is a stratified tissue, composed of 3 cellular and 2 acellular layers, the structural organization of which is optimized for optical transparency and any damage to this tissue can cause change or loss in vision (Figure 1.1).

The cornea can be divided into three main cellular compartments: the outer epithelium, the stroma, which is populated by keratocytes, and a single cell layer endothelium. On the interface of each of these layers reside two specialized acellular zones: Bowman's layer (8-16μm), which is found at the epithelium/stroma interface, and a Descemet membrane (3-5μm) at the stroma/ endothelium interface (Figure 1.2)[3].

The epithelium comprises 10% of the cornea's total thickness. It contains five to six layers of epithelial cells in the center and about eight to ten layers in the peripheral cornea – the limbus[4]. The presence of tight junctions throughout the epithelial surface

1

creates a tight barrier that restricts movement of molecules between cells [4] and therefore, prevents excessive evaporation from the cornea and maintains its hydration (Figure 1.1 and 1.2 (b)). The outer surface is lubricated by the tear fluid, which is constantly secreted and the excess is discharged through the tear ducts and into the nasal cavity. The epithelium is under a constant state of regeneration and has an eleven day cycle that starts with the proliferation of the epithelial cells (cell division and mitosis), then a process of motility and migration from the periphery to the center, and ends with their differentiation and stratification [4].

Underlying the epithelium is a specialized zone, called the basement membrane that serves as the demarcation between epithelial cells and the stroma. It contains collagen IV, laminin, fibronectin, vitronectin, and heparan sulphate proteoglycan [5]. These proteins interact with the basal epithelial cell membrane bound integrins which in turn interact with cellular actin through a cascade of cytoskeletal proteins like: talin, vinculin and α-actinin (Figure 1.1) [5] This produces stable adhesions between the basal epithelial cells and the extracellular matrix [5], and is thought to regulate cell shape, proliferation, migration, and differentiation [1].

The stroma comprises about 90% of the cornea's total thickness and is densely packed with highly organized proteins that form the extracellular matrix, through which the cells from the epithelium and stroma are connected [6], and organized in their individual locations on either side of the Descemet's and Bowman's Membrane [5]. The function of the stroma is to provide strength to the cornea, and protect the inner eye

structures from penetrating mechanical injuries. The stroma is also a regenerative tissue layer that is capable of repairing itself. The main ECM proteins are Collagen I, III, and glycosominoglycans (GAGs, keratin sulphate, hyaronic acid, and chondroitin sulphate). The collagen fibrils in the ECM are uniformly organized in parallel in a lamellar arrangement and are stabilized at fixed distances by proteoglycan covalent cross-linking [6]. The keratocytes in the stroma are responsible for collagen and GAGs synthesis, and are in turn found in the same parallel orientation as the collagen fibrils (Figure 1.2 (c)). Therefore it is hypothesized that the corneal stroma's structural and mechanical properties in terms of tensile strength, ECM and cell arrangement arise from the parallel alignment of collagen fibers. In addition, the lamellar arrangement of collagen fiber sheets is resilient to penetrating injuries. It is important to note that the parallel layers of cells and collagen are in alternating orthogonal orientation and this together with collagen's inter-lamellar distances are the features that are considered to be responsible for the optical transparency of the cornea [3, 4].

The endothelium, in humans, is a single cell layer that does not regenerate past a certain age. The cells at the center tend to be tightly packed in an even distribution and have a hexagonal morphology, whereas at the periphery, the cells are more spread out and of irregular shape. The cells are attached to each other through ocludins, which are junctional protein complexes [4]. Throughout the surface of the endothelium are ion pumps (e.g. sodium-potassium ATPase) that transport water, ions and nutrients from the aqueous humor fluid component of the anterior chamber through the stroma and to the epithelial

cells. As a result, its main function is to control the level of hydration in the cornea, and therefore regulate thickness, visual acuity, and transparency [4].

Collagen structure and function

There are twenty types of collagens known to date [7, 8]. The most prevalent are fibrillar collagens types I, II, III; which provide mechanical stability and strength, and type IV which tends to be an intermediate between febrile and globular. Type I is also the most abundant; it is the main component in bone and tendons, type II is found in cartilage, type III usually accompanies type I for reinforcement, and type IV, the foundation of basement membranes [9] . Collagen in the stroma is mainly type I and a small percentage of type III. It is made up of three polypeptide α-chains, which are a product of two genes that produce one α1 (Col I α1) and two α2 (Col I α2) chains. Each chain is wound into a left-hand helix and all three are then wrapped around each other and stabilized through hydrogen bonds in a right-hand sense to form a triple helix [10 9] . The enzymes that mediate the formation of these cross links are prolyl-hydroxylase and lysyl-oxidase. The peptides have a repeated amino acid sequence of Glycine-X-Y, where X is Proline and Y is hydroxyproline and sometimes hydroxylysine (Figure 1.3 (a)). This is an excellent example of how the primary sequence of a protein dictates its structural function. Glycine is a small amino acid with only hydrogen in its R group. Its presence in every third position of the protein provides the flexibility necessary to pack the triple helix through all its conformational changes with minimum strains. Proline has a rigid cyclic R group that forces the chain to wind up in a specific direction therefore

4

contributing to its stability. Hydroxyproline also provides stability to the chain through its hydrogen bonds [10] [9].

Collagen I α1 has about 1056 amino acids; of these 1014 amino acids are in the triplet sequence mentioned above. Sixteen amino acids on the N terminal and twenty-six on the C terminal of this chain are part of non-triplet regions called telopeptides [11]. Collagen I α2 chains, are composed of 1038 amino acids, 1014 of them are also in the triplet region, where the N terminal telopeptide has nine amino acids and fifteen in the C terminal. The function of the telopeptides is still unknown [11].

Collagen undergoes extensive processing during its synthesis (Figure 1.3 (b)). It starts with the specific transcription of α1 and α2 genes forming the pre-mRNA followed by its translation. In the next processing step, the basic collagen unit, called the procollagen, undergoes several intracellular modifications such as: removal of pro-peptides, hydroxylation of prolines and lysines, glycosylation of hydroxylysines, hydrogen bonding and protein folding into the triple helix, also known as the tropocollagen at this stage. Tropocollagen is then transported by secreting vesicles that are attached through the leading peptide and telopetides, to the extracellular matrix where it undergoes further extracellular processing by proteolytic cleavage to the active collagen fibril form, and deamination of the lysine residues to form the cross-links between the fibrils [10, 11].

Significance and Importance of Tissue Engineered Corneas

The significance of reproducing a fully functional bio-engineered cornea is to meet the growing needs and demands for cornea transplants [12, 13-18]. It has been reported by the World Health Organization that the leading causes of vision loss and blindness are corneal diseases, and corneal scarring [12, 19]. Keratoconus, corneal dystrophies, penetrating injuries, chemical burns, intraocular pressure (IOP) lowering treatments (trabeculectomy), and cataract surgeries all damage the cornea and lead to cornea transplants.

Rabinowitz and Hu [20, 21] define keratoconus as a non-inflammatory corneal ecstasies linked to stromal thinning, iron deposition in the epithelial basement membrane, and breaks in the Bowman's layer [2, 20]. Thus, the function of the cornea is impaired due to a reduction in protein content, making it thinner and softer than normal and as a result, bulges and increases its curvature. Extensive research is currently underway to understanding this phenomenon; some researchers suggest that it is due to mutations or abnormalities in the enzymes responsible for the lipid peroxidation and nitric oxide pathways [22], while others believe that it is due to a malfunction in the cornea's ability to organize and arrange collagen fibrils in their correct lamellar orientation [23]. Current treatment involves adjusting visual acuity through rigid gas permeable (RGP) contact lenses and corneal surgeries such as keratoplasty; however this increases the risk of corneal scarring and might exacerbate the initial condition and lead to the need for cornea transplants.

Corneal dystrophies are a group of corneal disorders that are genetically inherited. They are characterized by being non-inflammatory, bi-lateral, and alter the cornea's transparency and refractive function, ultimately obstructing vision [24]. There are several types of corneal dystrophies which make diagnosis for this disorder challenging, however they can be classified according to the location of the affected area: anterior membrane (epithelium), stromal, and endothelial. In endothelial dystrophy, for example, the aqueous humor leaks to the cornea causing edema, scarring and in extreme cases corneal ulceration. Initial treatment involves eye drops to relieve the edema; advanced cases require keratoplasty or corneal transplants [25].

Trabeculectomy, also known as filtration surgery, is a common surgical procedure that helps reduce the intra-ocular pressure (IOP) in the eye. A small incision "flap" is made between the sclera and the conjunctiva, thereby forming a new reservoir "bleb" for the excess aqueous humor to drain, and relieve the high IOP [26, 27]. In practice, this is an efficient and practical method to treat high IOP (glaucoma), however complications in resealing the flap cause corneal scarring, and beyond the corrections that can be made to fix this problem, there has to be a corneal transplant.

Corneal damage like these and many others place a lot of pressure on Eye Banks to supply corneal tissue and an even higher pressure on finding the appropriate donors. As a result many alternatives to corneal transplants have emerged in the last three decades and are still under extensive research:

Refractive surgery has been a popular procedure for the correction of refractive errors. These include redial keratotomy (RK), photorefractive keratectomy (PRK), laser-assisted in situ keratomileusis (LASIK), and laser-assisted sub epithelial keratomileusis (LASEK) [12]. The oldest type of refractive surgery is RK, which has been around for almost three decades. The procedure performs several incisions on the anterior segment of the cornea causing it to flatten and correct for different levels of myopia [28]. However, this method slowly declined in popularity as more efficient technologies emerged to improve visual acuity. The introduction of the laser in refractive surgery quickly became the option of choice since it provided great precision and accuracy in its incisions. PRK uses ultra-violet excimer lasers to perform clean cuts; the energy in the beam has the ability to break intermolecular bonds in the cornea thereby adjusting visual acuity exactly where it is needed [28]. Complications in this method include: post-operative pain, dry eye, stromal haze, and stromal scarring.

LASIK involves using a precision surgical instrument (microkeratome) to create an incision "flap". Computer generated topographical maps are then connected to a laser beam to carefully outline the cornea tissue that needs to be removed for correction. Once this process is complete the flap is replaced back to its corrected position (Figure 1.4). The advantages of this method over PRK are that the procedure eliminates the disruption of Bowman's membrane and epithelium and in addition to more efficient wound healing process, it is also reliable, and involves reduction in the use of extensive machinery [12, 28]. However, poor replacement of the flap prevents proper adhesion and might cause

infection and inflammation to the cornea, which subsequently introduces more distortions to the cornea's visual acuity[31], especially night vision, and complicated corneal scars leading to the need for corneal transplants.

Synthetic corneal onlays and inlays are also alternatives to corneal transplants that do not require great surgical procedures like LASIK and PRK. They are types of implantable lenticels placed on specific locations underneath the epithelium for onlays [12], or within the corneal stroma for inlays [12]. Corneal onlays, for example, alter the curvature and thickness of the cornea, but they do not provide good vision, as they are still in experimental stages, and only useful in extreme cases [12]. Intraocular lenses (IOL) are used to treat cataract, and even though they are not implanted in the cornea; they are placed in very close proximity to the epithelium (~mm) and any slight error in positioning IOLs will distort the epithelium and have severe consequences on the cornea's function[28].

Tissue Engineered Corneas To-Date

Bio-engineered corneas are the newest approach to finding solutions to the inadequate supply of tissue. To date, there is no complete corneal equivalent that can be used in clinical studies however researchers strive to find the means to accomplish this goal.

Extensive work is currently concentrating on finding the ideal artificial polymer or scaffold that will mimic the structural and mechanical properties of the cornea - principally collagen and GAG substitutes. The Myung group [15, 29] recently published a

review article on the use of various polymers and designs being investigated to accomplish this. Poly (methyl methacrylate) (PMMA) is one of the most popular polymers used commercially for ocular integration; it is a transparent, bio-stable plastic that has the ability to support visual acuity. It's most common uses is in the manufacturing of contact lenses and IOLs, however it is impermeable to water and nutrients and as a result lead to dry eye syndromes. Many complications arise for that same reason when designing a keratoprosthesis using PMMA such as retroprostheic membrane formation, glaucoma, extrusion, endophthalmitis, and rejection [29-31]. A lot of work on PMMA is focusing on integrating the polymer with more permeable bio-materials to overcome the complications mentioned above [29].

The AlphaCor keratoprosthesis, developed by the Hicks groups [32], is a poly (hydroxyethyl methacrylate) (PHEMA) hydrogel manufactured in a "core-and-skirt" design. Its success is attributed to the fact that it is the first hydrogel to give promising *in vivo* results for bio-integration as an artificial cornea in rabbits. PHEMA is more water permeable, porous and mechanically stronger than PMMA, however; it still has low permeability to glucose and nutrients which prevents correct epithelialization in the cornea [29]. In addition, its hydrophobic nature makes it vulnerable to protein adsorption and possible calcification (catastrophic failure) of the cornea [29]. Research is also being conducted to integrate "cell-adhesion promoting elements" to promote epithelialization and growth [29, 33].

Myang et al.[15, 29] also adopt the "core-and-skirt" design by using an integration of poly (ethylene glycol)/ poly (acrylic acid) (PEG/PAA) in an "interpenetrating polymer network" to sustain a foundation for epithelialization in the "core", and a micro perforated poly (hydroxyethyl acrylate) (PHEA) "skirt" that will support bio-integration in the stroma [15, 29]. The PEG/PAA copolymerization combines the biocompatibility, wettability, and mechanical strength of PEG with the hydrophilic nature, high absorbency, and miscibility of PAA to produce a hydrogel with mechanical and physical properties comparable to that of the cornea. The hydrophilicity of the hydrogel may provide the polymer with a resistance to protein adsorption but this compromises the ability of the hydrogel to support cell adhesion and growth. Myang et al.[15, 29] are currently trying to solve this problem by coating the hydrogel with collagen type I solution. This model shows a lot of promise, but its bio-compatibility, optical and mechanical properties still need to be optimized before *in vivo* studies can be attempted [15, 29].

Other polymers that are studied include: poly (vinyl alcohol) (PVA) [34, 35], and Poly (glycolic acid) (PGA) [13].

Some biomedical engineers and biomaterials scientists have redirected their interests to studies and characterizing nanofibers as scaffold components that will mimic the 3-dimensional tissue matrix [24, 36-39]. The goal of this new strategy is to provide a suitable environment in which cells can interact with each other and with the ECM for complete tissue function. Electrospinning is a novel fiber production process that entails

using polymer solutions that is expelled through a positively charged capillary tip to produce long micro and nano-fibers, which are captured on negatively charged collectors. The polymer will jet out the capillary tip once the electrostatic forces between the tip and grounded target are larger than the surface tensions of the polymer (or collagen) [36]. Many polymers have been evaluated as candidates for electrospinning including: poly (glycolic acid) (PGA), poly (lactic acid) (PLA), polydioxanon (PDO), collagen, elastin, gelatin, fibrinogen, in addition to different mixes of polymers at different ratios and concentrations [36]. Electrospinning is a feasible process that can produce long, aligned fibers of known dimensions and can be controlled. However, despite this flexibility, the smallest fibers manufactured are still larger in diameter than the normal range found in tissues (50-500nm) [36]. Furthermore, the inability to cross-link the aligned fibers limits the mechanical strength of these polymers, which imposes a challenge for researches to generate a viable tissue scaffold [36].

Another aspect of cornea modeling is focused on using collagen I instead of artificial polymers as the main scaffold to mimic the cornea's ECM. Collagen I is the most abundant protein in mammals and is the main component in the corneal stroma, therefore; it seems logical to use it in an artificial cornea and design a construct that will resemble the cellular and tissue organization present in the cornea. Germain et al.[5] presented a review article in 2000 that described the ideal methodologies for cornea construction which entailed four main steps [5]:

1. Isolation, culture, and expansion of each cell type separately in culture flasks.

12

2. Production of the stroma (in this case, using collagen as the substrate)

3. Reconstruction of the epithelium

4. Addition of the endothelium.

The most challenging of these steps is producing the stroma; because the scaffold must be bio-stable, porous, permeable, tensile, and provide a suitable environment for cell adhesion, proliferation, and repair; but it must also be organized in a homologous fashion to the lamellar arrangement observed in the corneal stroma that supports the cornea's transparency. Germain et al.[5] discuss these challenges in depth and pave the road for future work, and for the past three decades investigators have been concentrating on understanding the different characteristics of collagen to design a realistic model of a corneal stroma.

Crabb et al.[14] and many others have done remarkable work on the mechanical and structural characterization of collagen sponges and hydrogels [14, 40-42]. The data presented by Crabb et al.[14] showed that both fibroblasts and epithelial cells adopted similar morphologies in collagen films to that observed in the cornea, and the fibroblasts embedded in the sponge produced collagen fibrils that were comparable in diameter (35-75nm), to the collagen fibrils found in the cornea (30nm) [14 43, 44]. Future work entails optimizing the optical properties, mechanical strength, and the feasibility of stacking the single films to regenerate the stroma.

Many other investigators focus their work on studying different means to control collagen alignment by collagen electrospinning [36, 36-39, 45]; induction by magnetic fields [3], cell sheet engineering [46, 47], and micro-patterned collagen films [48].

In our lab, Dimitrijevich et al. have done extensive work on modeling the ocular tissue and have constructed several variants of corneal equivalents that have been patented [4, 49-53]. They have designed protocols to produce non contracting ECM equivalents that are transparent and provide subtle environment for cell attachment, migration, and proliferation. They use acid soluble collagen type I, which, once neutralized becomes temperature sensitive and gels at $37^{\circ}C$[50]. The protocols that were designed represent 3-dimensional *in vitro* models for the tri-cellular compartments in the cornea: the epithelium [50-52], stroma [49, 50], and endothelium [50, 53]. However, the stroma matrix is unorganized and the corneal stromal fibroblasts are in a random fashion.

With this, **we hypothesize that collagen organization directs cellular organization in the corneal stroma and controls its function.** This will be demonstrated by first, testing whether the cells in the cornea exit the tissue in the same *in vivo* organization independent of collagen organization *in vitro*. Secondly, it will be shown that the cell arrangement is in fact dependent on ECM organization. In the next step, we will test the feasibility of constructing a model that will mimic the collagen organization and thus direct cellular organization in the cornea stroma.

Figure 1.1: A representation of the cornea in the eye, the cellular compartments, and the protein interactions in the basal membrane.
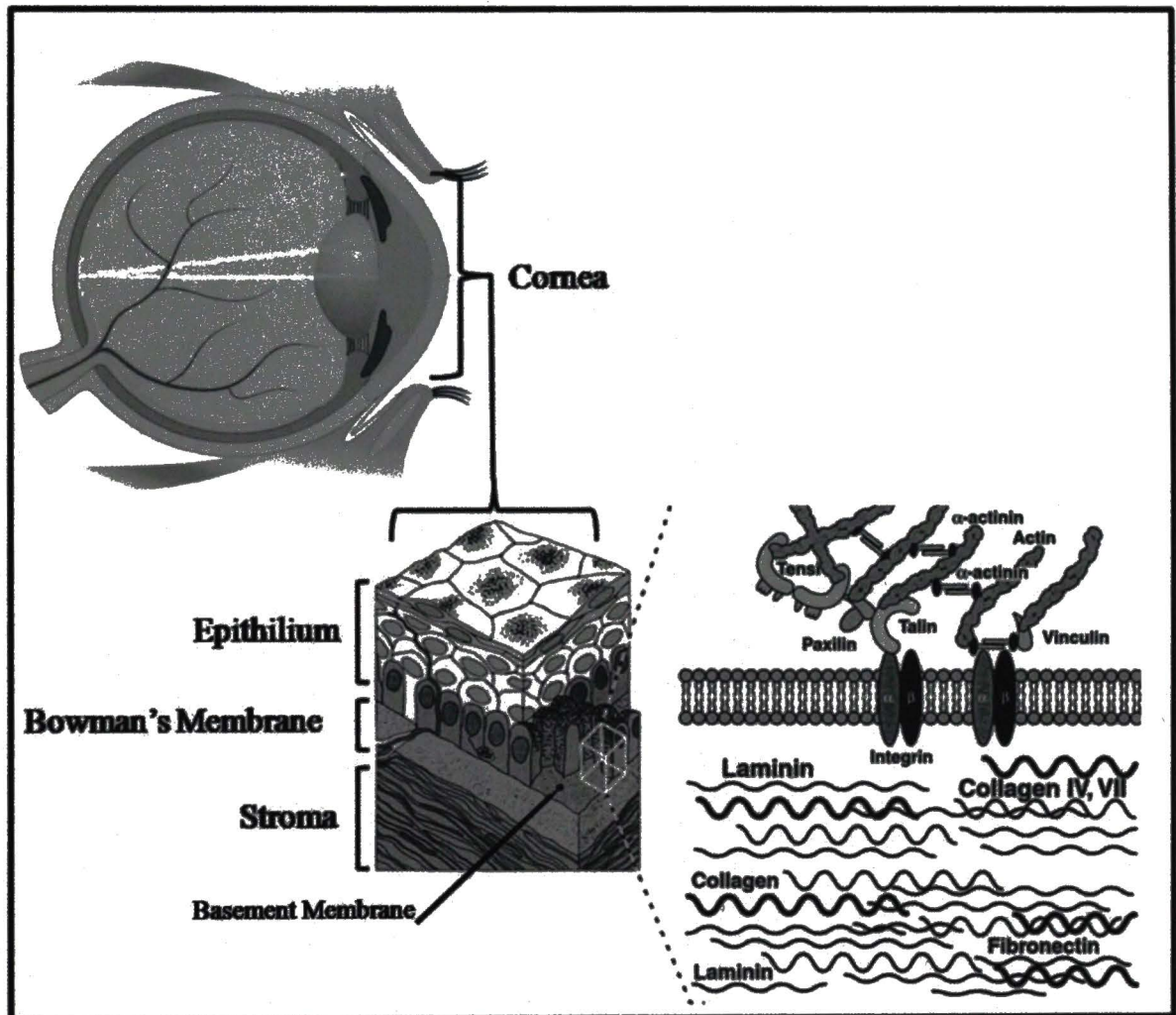
Figure 1.2:

(a) Complete representation of the cellular and acellular compartments of the cornea.

(b) Representation of the corneal epithelium.

(c) Representation of corneal stroma.

(d) Representation of the corneal endothelium.

(a)

- → Epithilium
- → Bowman's Membrane
- → Stroma
- → Descemet's Membrane
- → Endothelium

(b)

- Epithilial Cells
- → Basement Membrane
- Bowman's Membrane

(c)

Collagen Fibrils in a
Lamellar Arrangement

Fibroblasts

(d)

Descemet's Membrane

Single Cell
Endothelium
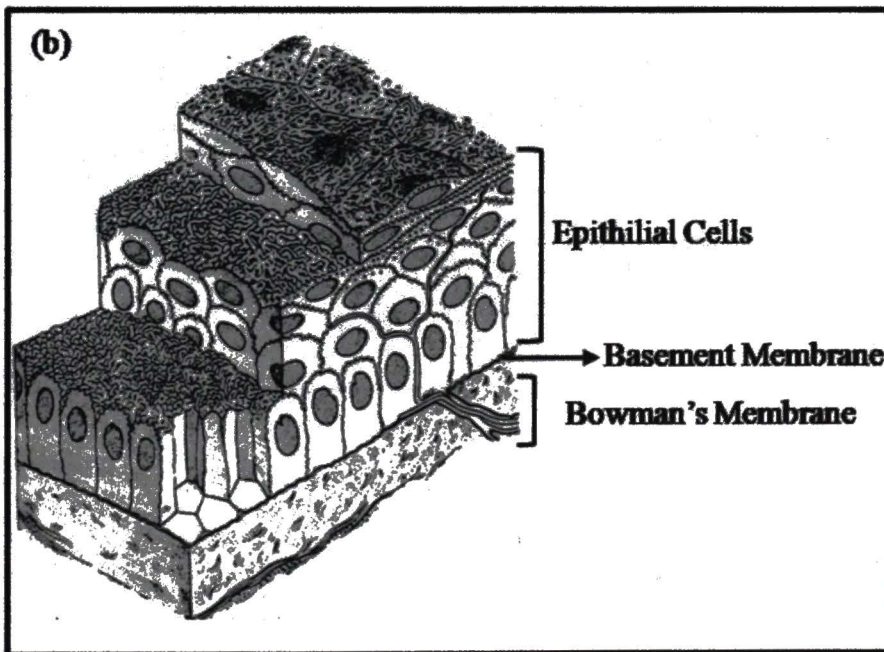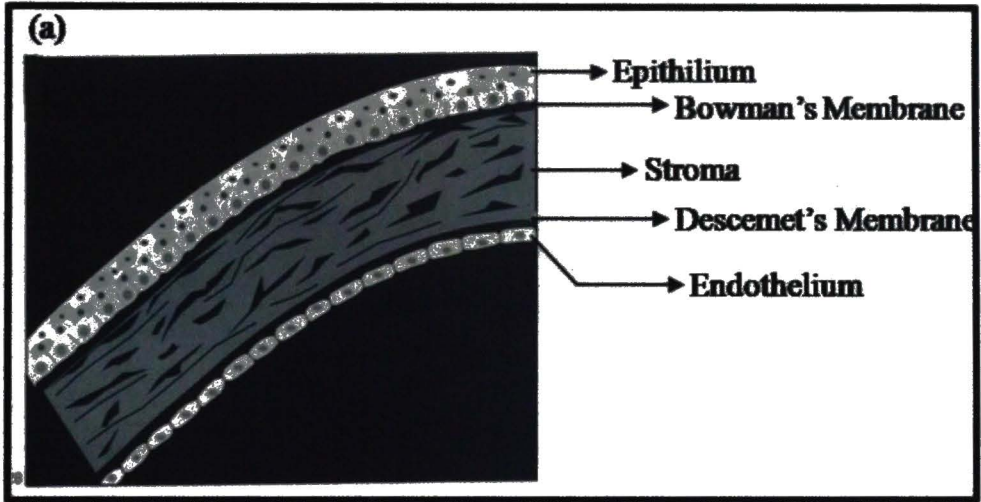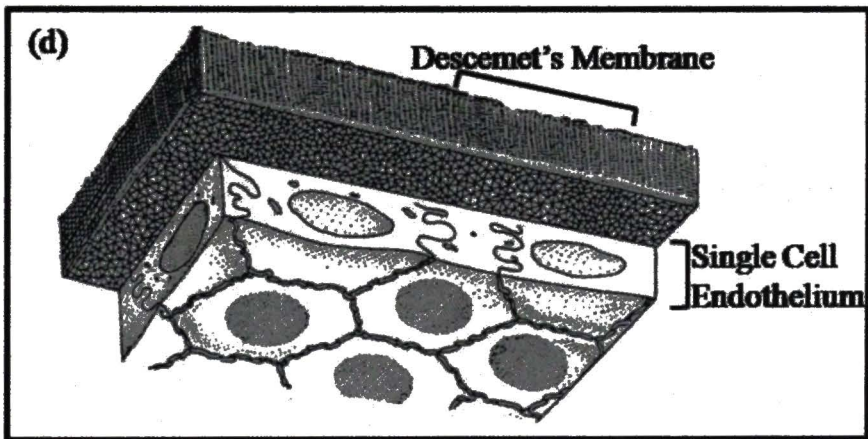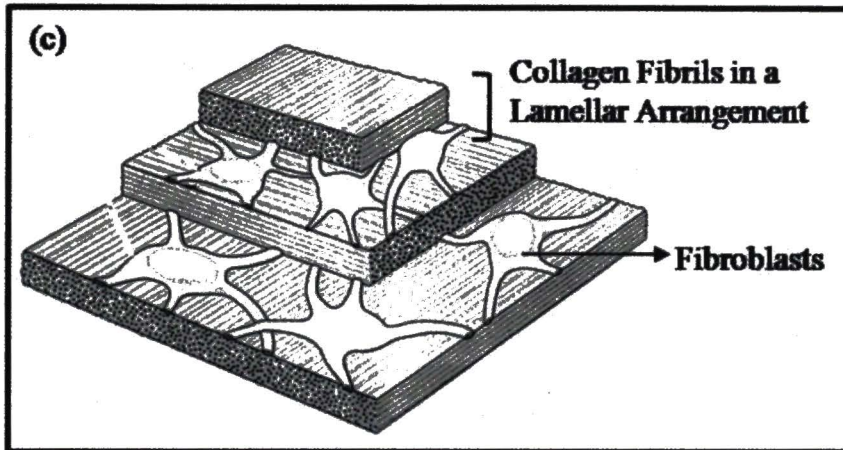
Figure 1.3:

(a) Primary and secondary structure of the collagen triple helix.

(b) Collagen synthesis in the endoplasmic reticulum, followed by its transport into the extracellular space, where extensive modification and processing takes place.

(a)

(b)

(1) Translation of mRNA collagen transcript

(2) Intracellular modification to Procollagen

(3) Protein folding into the tropocollagen triple helix

(4) Secretion from cell

(5) Extracellular modifications of tropocollagen: cleavage of N and C terminus, and deamination
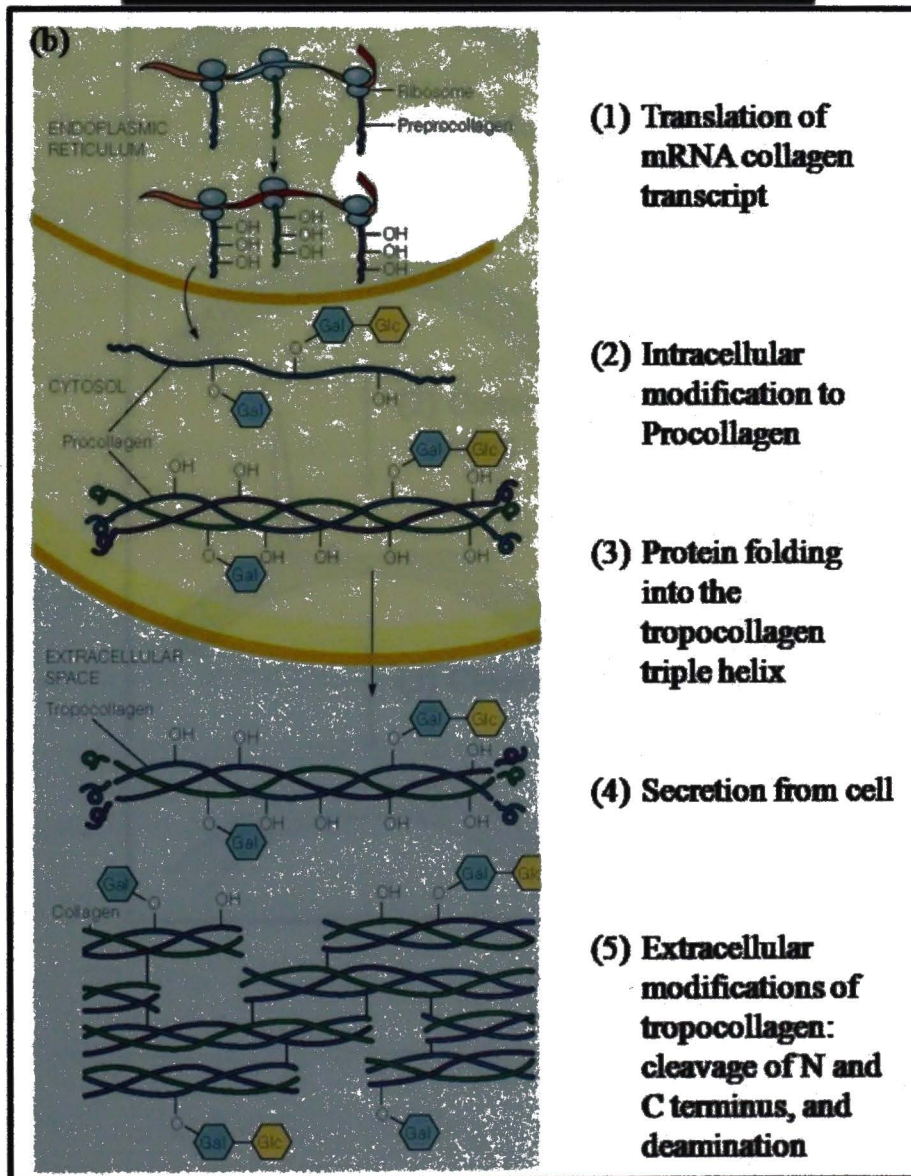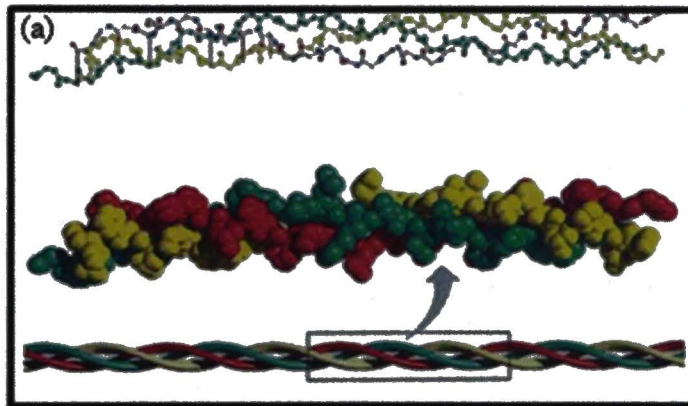
Figure 1.4: Schematic representation of LASIK procedure

(1) Create an incision "flap" using a microkeratome.

(2) Correct for refractive error.

(3) Close incision "flap"
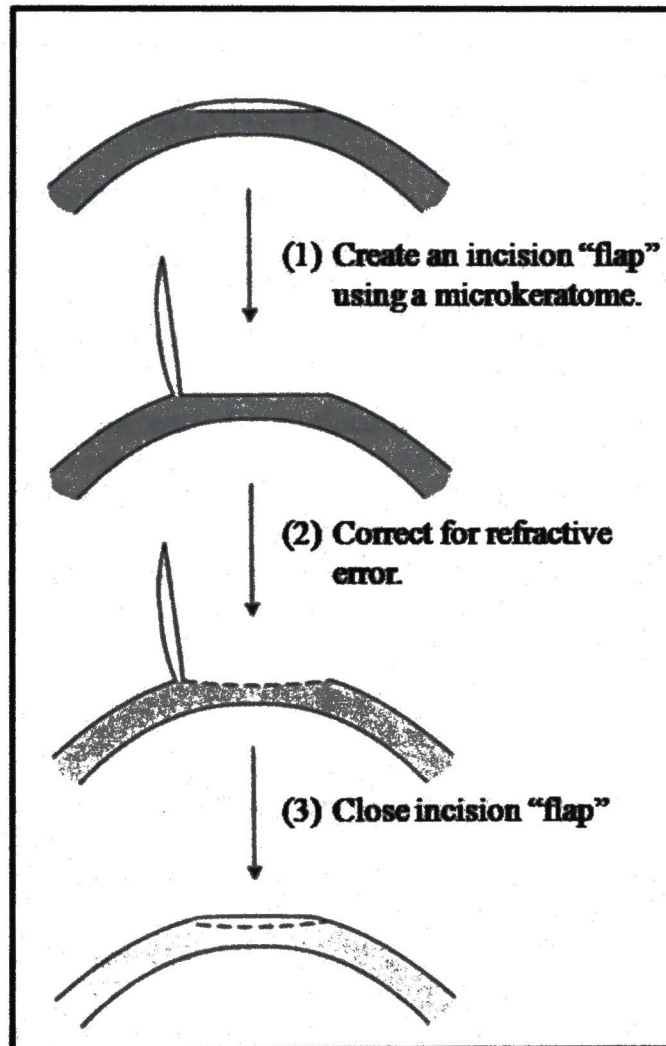
CHAPTER II

DEPENDANCE OF CELLULAR ORGANIZATION ON COLLAGEN

ORGANIZATION IN CORNEAL STROMA

Collagen is the most abundant protein in our body; it is the main matrix component in bone, cartilage, tendons, and skin. Its known molecular structure and supramolecular organization is key to its function, and its organization in each tissue is related to its environment and tissue function. However, it is not clear how this distribution is controlled by the cells and other ECM components. Do the cells that synthesize the collagen control its organizations? And does organization control cellular function?

Specific Aim 1:

Test if the cells in the cornea exit the tissue in the same organization fashion as it is *in vivo*, independent of collagen organization surrounding the tissue *in vitro*.

Rationale and Experimental Design:

The question under study is whether or not the ECM controls cell distribution in the cornea, or vice versa. It is known that the collagen fibrils are aligned in parallel and are linked together through lamellar cross-links at fixed lamellar distances. It is also known that the concentrations and locations of the other ECM components vary from

tissue to tissue and may dictate the structure of the corneal stroma. However, it is unclear whether the orientation and alignment of stromal fibroblasts is reason or consequence of ECM organization.

To test this, human corneal stromal biopsies (buttons) will be immersed in acellular collagen and the movement of the cells from the cornea button to the new collagen matrix will be monitored by phase contrast microscopy. Assuming that collagen does not control the spatial arrangement of the cells, it is expected that the cells will migrate out of the cornea in the same orientation as they are in within the cornea button. However, if collagen does control the spatial arrangement of the cells, then it is expected that the cells from the corneal stromal biopsies will migrate into the acellular collagen in a randomized fashion. This is because the collagen fibers in this new matrix are unorganized and are not arranged in the fixed inter lamellar distances.

MATERIALS AND METHODS

Corneal stroma biopsies: Corneal stromas were obtained from Eye Bank corneas. The epithelial sheet was removed by incubating the human corneas with dispase (BD Biosciences, San Jose, CA) diluted with calcium free EpiLife (12 units/Ml) at 4° for 48 hours as previously described[50-52]. The endothelium was then peeled off by removing the Descemet membrane and leaving totally denuded stroma [50, 51, 52, 53]. Punched biopsies (3mm in diameter) were then obtained from the stroma. These biopsies were then immersed in neutralized solution of bovine collagen type I (0.5mLs) in a 12 well plate, prepared as described below*. The 12 well plate was carefully placed in the incubator (37°C, 5% CO_2) and collagen allowed to gel. After collagen fibrillogenesis was complete, the model was cultured in HAMS F12 medium containing 5% fetal bovine serum (FBS), and incubated at 37° with 5% carbon dioxide (CO_2)[50, 52, 54]. Incubation was continued, and the 3-D culture monitored daily under phase contrast microscopy. After approximately 10 days, the corneal stromal fibroblasts began to emerge from the stromal biopsies and migrate into the collagen gel. At day 20, the corneal stromal fibroblasts were determined to completely populate the collagen matrix. The respective collagen gels were then washed, fixed (4% formaldehyde), dehydrated, then paraffin embedded and sectioned as described on page 25.

*Collagen preparation: 8 parts of solution bovine collagen type I at a concentration of 4mg/mL (calf skin, MP Biomedcals) was mixed thoroughly, with 1 part 10x HAMS F12

24

medium, and neutralized with 1 part reconstitution buffer (0.05N NaOH 1N, NaHCO$_3$, HEPES) while keeping all ingredients in ice (4°C) and avoiding generation of air bubbles[50, 51, 54]. Once the mixture was homogeneous, the pH was adjusted to 7.4 using pH indicator paper. The corneal biopsies were then immersed in 0.5mLs of the collagen mixture in each well of a 12 well plate as described above, and allowed to polymerize in a 37°C incubator with 5% CO$_2$. After collagen polymerization, the biopsies were treated with 1x HAMS F12 containing 5% FBS as described above and incubated at 37°C.

Paraffin sectioning: the collagen matrix containing the corneal stromal biopsies, as described above, was fixed in 4% formaldehyde overnight at 4°C. The formaldehyde was then removed and the sample was washed with distilled water 3x for 30 minutes in 4°C, and placed in 70%, 80%, and then 95% ethanol overnight at 4°C. The sample was then placed in a 1:1 ratio of ethanol and xylene for 1 hour, followed by 1 hour of 100% xylene, 1 hour of 1:1 ratio of xylene and paraffin, and 3x 1 hour washes with 100% paraffin. The sample was sectioned (~10μm) and treated with hematoxylin and eosin stain (H&E) [50, 52, 54].

Image acquisition: corneal stromal biopsies cultured in collagen, and H&E sections were examined under an Olympus AX70 phase contrast microscope using SPOT Twain software.

RESULTS

Cornea biopsies

The corneal stromal biopsies are shown in Figure 2.1 (a). The outgrowth of the stromal fibroblasts was observed under phase contrast microscopy. The cells started exiting the tissue and migrating into the acellular collagen matrix at day 10. Micrographs that were recorded at day 10 and after show random arrangement of the keratocytes in the acellular collagen (Figure 2.1 c, d, & e). Once significant populations of cells have invaded the acellular collagen matrix (up to day 20), the collagen and the corneal stromal biopsy was fixed, paraffin embedded and sectioned as described previously and treated with hematoxylin & eosin (H&E) stain (Figure 2.1 (b)). The keratocytes in the collagen matrix are in a random distribution and the acellular collagen is less dense than the stromal ECM.

Figure 2.1:

(a) Photograph of corneal stromal biopsies (3mm in diameter).

(b) Hematoxylin and eosin stain cross section of the fibroblasts exiting the stroma into the acellular collagen at 20x magnification.

(c) Fibroblasts exiting the stroma into the acellular collagen at 4x magnification.

(d) Fibroblasts exiting the stroma into the acellular collagen at 10x magnification.

(e) Fibroblasts in the acellular collagen away from the cornea biopsy at 4x magnification.

(a)

(b)

200μm

(c)

2.0mm

(d)

500μm

(e)

2.0mm
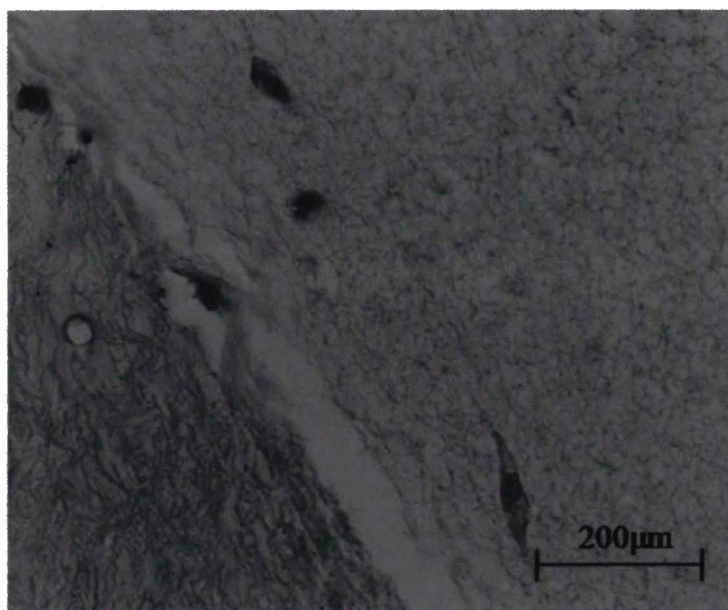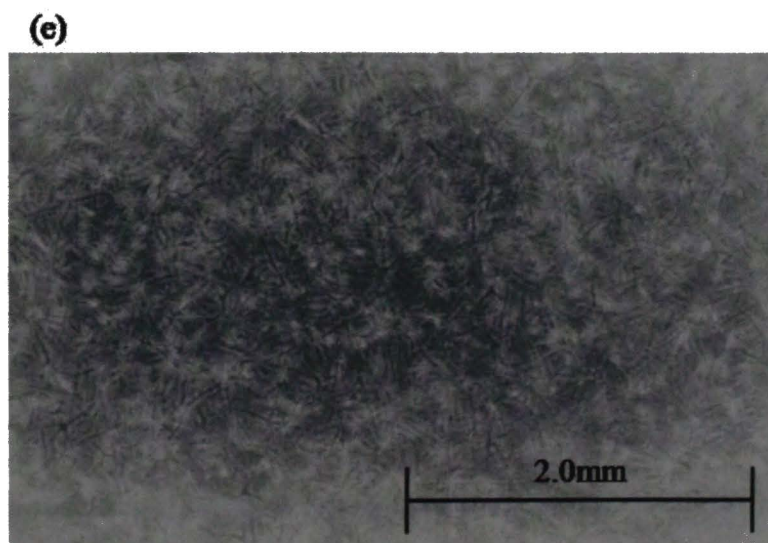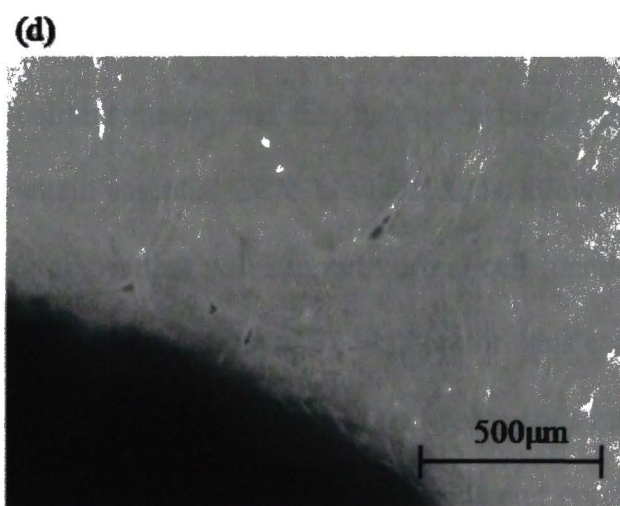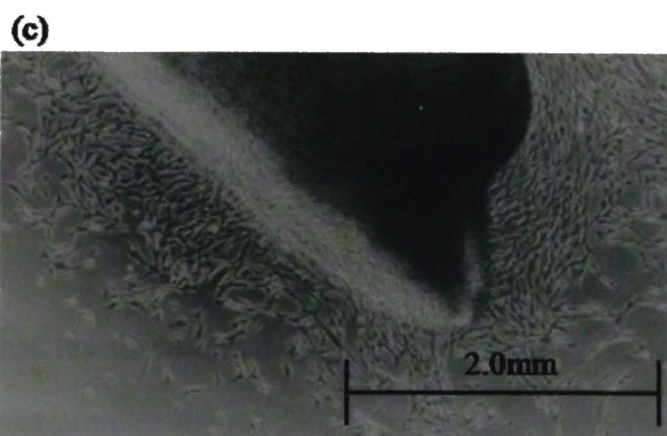
CHAPTER III

DESIGNING AN ARTIFICIAL CORNEAL STROMA CONSTRUCT

The approaches discussed in Chapter I concerning engineering a viable corneal replacement hold great promise for the future, however in order for this to materialize several factors must be considered. The construct must be made using a biomaterial that can serve as the extra-cellular matrix and that can be fashioned into a lens for vision corrections. It should contain essential ECM bio-molecules, allow free access to growth factors, nutrients, and cytokines that will support normal cell function, and be hydrated. Collagen is the most abundant protein in the ECM; therefore this can be used to serve as a model of the authentic corneal stroma matrix. Type I collagen is readily available for *in vitro* studies, the most commercially accessible are bovine and porcine collagen, and we have shown that human stromal fibroblast and epithelial cells can be cultured in and on them. It has also been shown that animal collagen may produce an immunogenic response in only a small percentage of individuals (~5%). This is due to the fact that the sequence and structural properties of collagen I are conserved across species and is not detected by the immune system as a foreign protein [11]. However, by virtue of its avascular nature, the cornea is considered to be an immuno-privileged tissue and this further reduced immune reactions. Collagen type I used for research is acid-solublized which is

used as a solution with a pH of 3.29 in hydrochloric acid. It is soluble at 4°C and once neutralized becomes temperature sensitive and gels at 37°C.

Collagen has the advantage of being able to form transparent gels that are bio-stable, tensile, and flexible. The gels can be molded into a desired size and shape, and are nutrient permeable. In several studies, fibrin and laminin have been added to the collagen matrix to improve mechanical properties.

Specific Aim 2:

Test the feasibility of constructing a model that will mimic the lamellar organization of collagen and thus direct cellular organization in the cornea stroma.

Specific Aim 2 (a):

Collagen can be fashioned into thin films and these can be stacked to resemble the corneal stroma lamellae and concurrently support higher cell densities than in a random collagen gel matrix.

Rationale and Experimental Design:

The questions under study here are:

(1) Can acellular collagen be assembled and engineered into sheets that can be stacked in layers to resemble the architecture of the corneal stroma?

(2) Is it possible to design the collagen sheet stacks to support large densities of viable cells that will remain in their lamellar arrangement, be permeable to growth factors and nutrients and keep the system viable for long periods of time?

(3)   Since arrangement is dependent on ECM organization; then is it possible to physically manipulate the acellular collagen matrix as to control the alignment of the collagen fibers in the thin film sheets, thereby paving an imprint for cell alignment?

Preliminary experiments with porcine and bovine collagen type I will determine which scaffold is a better candidate for the cornea construct. Seeding increasing cell populations on each collagen layer and testing the ability of the system to sustain the cells and keep them viable can accomplish this. Increasing the number of collagen layers on the stack will challenge collagen from each source. The corneal stroma is composed of about 200 to 250 lamellae. It is beyond the scope of this project to try to replicate this number of lamellae, because it would be impractical to generate the film thickness that would allow such precision in reproducing the corneal stroma. However the goal is to test a strategy that can mimic organization seen in the corneal stroma matrix. Therefore, if the proposed model can sustain 10 or more films of collagen and cells and remain viable then the strategy can be considered successful. Finally, the cells should be in a uniform and organized distribution throughout as to conserve the optical properties of the construct. To mimic the cell organization and alignment in the cornea, the cells must be arranged between consecutive lamellae; which would require control of cell orientation. Furthermore, the directional cell alignment in each layer of the stack should be orthogonal to the adjacent layers.

Confocal microscopy will be used to visualize the viability and density of cells in each layer. The cells will be labeled with alternating stacking of non-specific green and orange fluorescence to track the collagen lamellae. It is crucial to use an efficient and reliable method to track the cells. The most effective method is to label the cells with fluorescent dyes with different emission wavelengths. The fluorescent label must also be a marker of cell viability to ensure that the system is functioning. The dyes that would be most appropriate for these tasks are Cell Trackers® that contain chloromethyl groups that react with thiols in viable cells in a reaction that is mediated via Glutathione-S-transferase. Glutathione (GSH) is a sulfhydryl tripeptide that maintains the redox state of thiols functions as an antioxidant and eliminates free radicals and oxidants from the cell when GSH is oxidized [55-57]. Therefore, in most cells GSH is a vital molecule that is very abundant (10mM) and its presence is a strong indicator of cell viability.

Cell Tracker Green®, also called CMFDA, is 5-chloromethylfluorescein diacetate [56]. CMFDA is cell membrane permeable and can easily diffuse in and out of cells. However, the dye remains non-fluorescent until it is cleaved by cytosolic esterases and then conjugated to GSH via glutathione-S-transferase, thereby cleaving the acetate and releasing the fluorescent product. The dye may react with GSH first, however the product will not be fluorescent until it is released by the esterases. Once the dye is conjugated to GSH it is transformed into a cell-impermeant fluorescent dye-thioether and remains inside the cell (Figure 3.1 (a)).

Cell Tracker Orange® is (5-(4-chloromethyl) amino) tetramethylrhodamine, referred to as CMTMR [56]. Its characteristics are similar to CMFDA in the sense that it moves freely across the cell membrane until it is conjugated to GSH. However, it does not require enzymatic cleavage by a cytosolic esterase; the reaction with glutathione-S-transferase is all it needs to release the fluorescent product.

These dyes are excited at wavelengths which are workable outside the UV range, which ensures that the collagen stack will not be affected by UV irradiation. The excitation and emission wavelengths of Cell Tracker Green® and Orange® are presented in Table 1.1 as well as their wavelength spectra in figure 3.1 (b) and (c). The fluorescence detector is usually equipped with two argon ion lasers; one excites the 360nm line and the other is tuned to the excitation wavelength of the desired dye under use, and then the emission is collected according to the dyes' emission wavelength [55, 57].

Table 1.1: Excitation and emission wavelengths of CMTMR and CMFDA.

Cell Tracker Probe	Excitation Wavelength (nm)	Emission Wavelength (nm)
CMTMR	541	565
CMFDA	492	517

Specific Aim 2 (b):

Determine if the expression of major cytoskeletal proteins in the stromal fibroblasts on the artificial collagen construct is similar to that of the corneal stromal fibroblasts in the corneal stroma.

Rationale and Experimental Design

When designing an *in vitro* cornea model it is important to study the expression of marker proteins that are specific to stromal fibroblasts (or other cellular components in the cornea). The construct should mechanically and structurally resemble the corneal stroma, and the corneal stromal fibroblasts in the construct should express the same proteins and respond to the same signaling stimuli *in vitro* as they do *in vivo*. Since morphology is key to the function of the fibroblasts in the cornea construct, well characterized cytoskeletal protein markers that are specific to the function of stromal fibroblasts will be used. For the purpose of this study α-smooth muscle actin (α-SMA), myosin heavy chain (MHC), myosin light chain (MLC), and vimentin (Vim) were chosen as proteins that characterize the fibroblasts' morphology. Their protein expression in the cornea construct will be demonstrated by indirect immunofluorescence.

There is significant evidence demonstrating that in response to wound healing and scar formation in the cornea, there is an increased expression of TGF-β which initiates the differentiation of fibroblasts to myofibroblasts as demonstrated by an increased expression of α-SMA [58]. α-SMA can then be incorporated into stress fibers and

35

together with the coupling of the ATP-dependent motor protein MHC; direct *in vivo* cellular contractility [58-60]. Myosin II is known to play an important role in cell motility in fibroblasts and is thought to be correlated with the expression of MLC [61]. Finally, unlike α-SMA, MHC, and MLC, Vim is an intermediate filament frequently expressed in fibroblasts that provides the cells with structural and mechanical integrity [62].

Specific Aim 2 (c):

Test the optical properties of the corneal stroma construct.

Rationale and Experimental Design

The optical properties of the cornea are of vital importance to its function, but are often overlooked when designing *in vitro* models or artificial constructs. The cornea is known to be optically active since it is able to transmit 98% of incident light between wavelengths of 400-700nm (visible region) [63], and has almost zero light scattering [44]. The cornea's lack of light scattering is thought to be due to the uniform refractive indices of ECM and cells in the stroma as well as the transparencies of the epithelium and the endothelium [44] [63]. Even though X-ray diffraction and SEM data show differences in the refractive index (birefringence) of the corneal components (corneal stroma ECM, corneal stroma fibroblasts, epithelium, and endothelium) [44], it seems that the collaborative organization of the collagen fibers in the ECM, corneal stromal fibroblast, and other components of the cornea, together with their fixed spatial arrangements form a structure that exhibits what is known as "constructive interference" [44]. Achieving the goal of

36

designing an artificial cornea involves reproducing as faithfully as possible this organization and preventing factors that cause "destructive interference" of the transmissible light. This will be demonstrated by measuring the percentage transmittance of the collagen stacks with and without cells. Optical activity will also be evaluated by determining the polarization of the collagen stack between two polarizers in the path of an incident beam and rotating the second polarizer at varying angles in reference to the first polarizer (figure 3.21). Incident light, which is unpolarized, is made up of electrical and magnetic energies that adopt multidirectional wave forms, and polarization reduces their oscillations into a single unidirectional wave form [64]. When incident light passes and transmits all the light through two polarizers, provided that both polarizers are on the same principal axis (0° and 180°), the light is said to be completely depolarized. When the second polarizer is perpendicular to the first polarizer (90° from the principal axis), an object is considered optically active if it completely blocks transmission of the light that passes through the first polarizer except through the object itself [64]. This is a good method that demonstrates the optical activity of the corneal stroma construct.

MATERIALS AND METHODS

Corneal stromal fibroblasts cell culture: Donor Corneas obtained from the Eye Bank were first decontaminated by incubation in DMEM containing 10% penicillin-streptomycin. Corneas were then de-epithelialized by incubation in dispase (BD Biosciences, San Jose, CA) diluted with calcium free EpiLife (12 units/Ml) at 4° for 48 hours as previously described [50-52]. The endothelium with the Descemet membrane were then removed from the posterior segment of the stroma as previously described[50, 50, 51, 51, 52, 52, 53, 53]. The remaining corneal stromas were dissected into 2mm cubes, placed in 6-well plates; they were then allowed to adhere for 1 hour in a 37°C incubator with 5% CO_2. The medium was then added (DMEM containing 10% FBS) was then added and corneal stromal fibroblasts were obtained as an outgrowth of the explanted stromal tissue. The cells were sub-cultured in tissue culture (TC) flasks with Dulbecco's Modified Eagles Medium (DMEM, Gibco) containing 10% fetal bovine serum (FBS) or HAMS F12 medium containing FBS (5%), in 37°C incubators with 5% CO_2. Cells were harvested using 0.05% Trypsin/EDTA (Gibco) and neutralized the enzyme activity with trypsin inhibitor [54]. Cells were then either used in experiment, sub-cultured, of frozen for storage.

Cell labeling: Corneal stromal fibroblasts cultured TC flasks as described above were allowed to proliferate to near confluence and were non-specifically labeled with fluorescent dyes, Cell Tracker Green® (CTG) and Cell Tracker Orange® (CTO) (Molecular Probes). The dyes were diluted in DMEM containing 10% FBS to a final

concentration of 0.05µM. 8mLs of the diluted dyes were added into the cell culture flasks and incubation continued overnight at 37°C with 5%CO_2.

Collagen preparation: 8 parts of solution bovine collagen type I at a concentration of 4mg/mL (calf skin, MP Biomedcals) was mixed thoroughly, with 1 part 10x HAMS F12 medium, and neutralized with 1 part reconstitution buffer (0.05N NaOH 1N, $NaHCO_3$, HEPES) while keeping all ingredients in ice (4°C) and avoiding generation of air bubbles [50, 51, 54]. The order of addition of ingredients is important and was as described above. Each addition was followed by a period of thorough mixing before the subsequent step. Once the mixture was homogeneous, the pH was adjusted to 7.4 using pH indicator paper and poured into Petri dishes as described below.

Corneal stroma collagen film stack: On day 1, sixteen 2cmx2cm glass cover slips and two 12x12cm^2 Petri dishes were rinsed in 100% ethanol and sterilized under UV for 2 hours as described in figure 3.2. The sixteen glass cover slips were set on the Petri dish and 10mLs of the collagen mix prepared as described above was poured onto the cover slips. A cell scraper was used to spread the collagen evenly in a single direction on the glass cover slips and the direction was noted. The Petri dish was incubated in 37°C for 2 hours, and then 15mLs of HAMS F12 containing 5% FBS were added and incubation continued overnight in 37°C incubator with 5% CO_2.

On day 2, the fluorescent corneal stromal fibroblasts labeled as described above were harvested using 0.05% Trypsin/EDTA (Gibco) and the enzyme activity was neutralized with trypsin inhibitor [54]. The cells ($1x10^5$ cells suspended in 100μL of media) labeled with each color fluorescence (green or orange) were seeded on cover slips in separate Petri dishes as shown in figure 3.2, and allowed to attach for 5 minutes after which 15mLs of HAMS F12 containing 5% FBS was added to each Petri dish, incubation continued overnight at 37°C with 5% CO_2.

On day 3, the thin collagen sheets bearing the fluorescently labeled cells were removed from the Petri dish using a scalpel, and cutting the edges around each individual glass cover slip as shown in figure 3.2. The glass cover slip were placed in another Petri dish containing HAMS F12 media, and were swirled gently until the thin collagen film peeled off the glass cover slip as shown in figure 3.2. Using two forceps, the thin collagen film was carefully carried onto a collagen sponge base where the stack is to be assembled. The protocol was repeated for every collagen film while alternating the growing stack with CTG and CTO cells until the stack was 20 films thick. 50μL of Fibronectin (FNC, Athena, Enzyme Systems) was added between the collagen films as the stack grew to act as adhesive "glue" and keep the layers from separating.

Immunocytochemistry: Corneal stromal fibroblasts (not labeled with CTG or CTO) cultured in TC flasks as described above were harvested and seeded on thin collagen sheets as described above, and allowed to attach overnight in 37°C incubator. The

40

collagen sheet bearing corneal stromal fibroblasts was then rinsed in phosphate buffer saline (1x PBS) (0.256g/L $NaH_2PO_4H_2O$, 1.19g/L Na_2HPO_4, 8.7g/L NaCl, pH 7.4) and fixed/permeabilized in methanol: acetone (1:1, 2hrs at 4°C), after which they were re-hydrated with distilled water and blocked (overnight at 4°C) in 1% BSA in PBS. Specimens were then rinsed with distilled water (3x) before incubation with primary (1°) antibody (overnight at 4°C). The specimens were then rinsed with 0.1% Tween 20 in distilled water (4x10mins) before incubation with secondary (2°) antibody (overnight at room temperature). The specimens were washed in 0.1% Tween 20 in distilled water (4x 10mins), and distilled water (4x 10mins), and finally mounted on glass cover slides after DAPI (4', 6-diamidino-2-phenylindole) staining (for 15 seconds in a concentration of 150nM) (FluorSave™, Calbiochem, La Jolla, CA) [54] [50-52].

Immunohistochemsitry: Corneal stromas prepared as described on page 38 were fixed in 4% formaldehyde overnight at 4°C. The formaldehyde was then removed and the sample was washed with distilled water 3x for 30 minutes in 4°C, and dehydrated with 70%, 80%, and then 95% ethanol overnight at 4°C. The corneas stroma was then placed in a 1:1 ratio of ethanol and xylene for 1 hour, followed by 1 hour of 100% xylene, 1 hour of 1:1 ratio of xylene and paraffin, and 3x 1 hour washes with 100% paraffin. It was then sectioned (~7μm) and deparaffinzed by placing the corneal stroma sections in 100% xylene 2x for 15 minutes each, followed by 100% ethanol 2x 15 minutes each, 75% ethanol 2x 15 minutes each, 50% ethanol 2x 15 minutes each, distilled water 2x 5

minutes each, 0.1% Tween in PBS 1x 5 minutes. The corneal stroma sections were then fixed with 4% formaldehyde overnight at 4°C and blocked (overnight at 4°C) with PBS + 1% BSA + 1% horse serum. Specimens were then rinsed with PBS (3x) before incubation with 1° antibody (overnight at 4°C). The specimens were then rinsed with 0.1% Tween 20 in PBS (4x10mins) before incubation with 2° antibody (overnight at room temperature). The specimens were washed in 0.1% Tween 20 in distilled water (4x 10mins), PBS (3x 10mins), and distilled water (4x 10mins), and finally mounted on glass cover slides after DAPI (4',6-diamidino-2-phenylindole) staining (FluorSave™, Calbiochem, La Jolla,CA)[50-54].

Antibodies: anti α-smooth muscle actin (α-SMA) (monoclonal in mouse, Sigma), anti-myosin light chain (MLC) (monoclonal in mouse, Sigma), anti-vimentin (monoclonal in mouse, Sigma), and anti-myosin heavy chain (MHC) (monoclonal in rabbit, Sigma) were used at recommended dilution in PBS.

Secondary antibodies were Alexa Fluor 594nm goat-anti mouse and Alexa Fluor 488nm goat-anti rabbit (Molecular Probes) and used at a 1:1000 dilution in PBS. Negative controls had only 2° antibody and showed no or minimum fluorescence.

Image Acquisition: Cornea constructs described above were examined under a Zeiss LSM 410 scanning laser electron microscope (X –Y – Z sections, and 3-D stack

assembly). Indirect fluorescence samples as described above were examined under an Olympus AX70 fluorescent microscope using SPOT Twain software.

Transmittance measurements: Percentage transmittance and absorbance of the cornea constructs were measured using Absorption Spectrophotometer 50 Bio Varian.

Figure 3.1:

(a) Esterase and Glutathione-S-transferase enzymatic action on CMFDA and cleavage of the acetate to release the fluorescent product.

(b) Spectrum of CMFDA (Cell Tracker Green®)
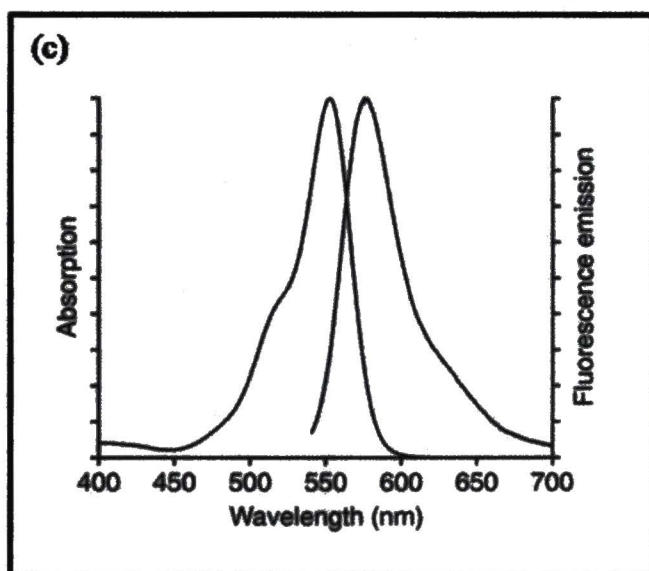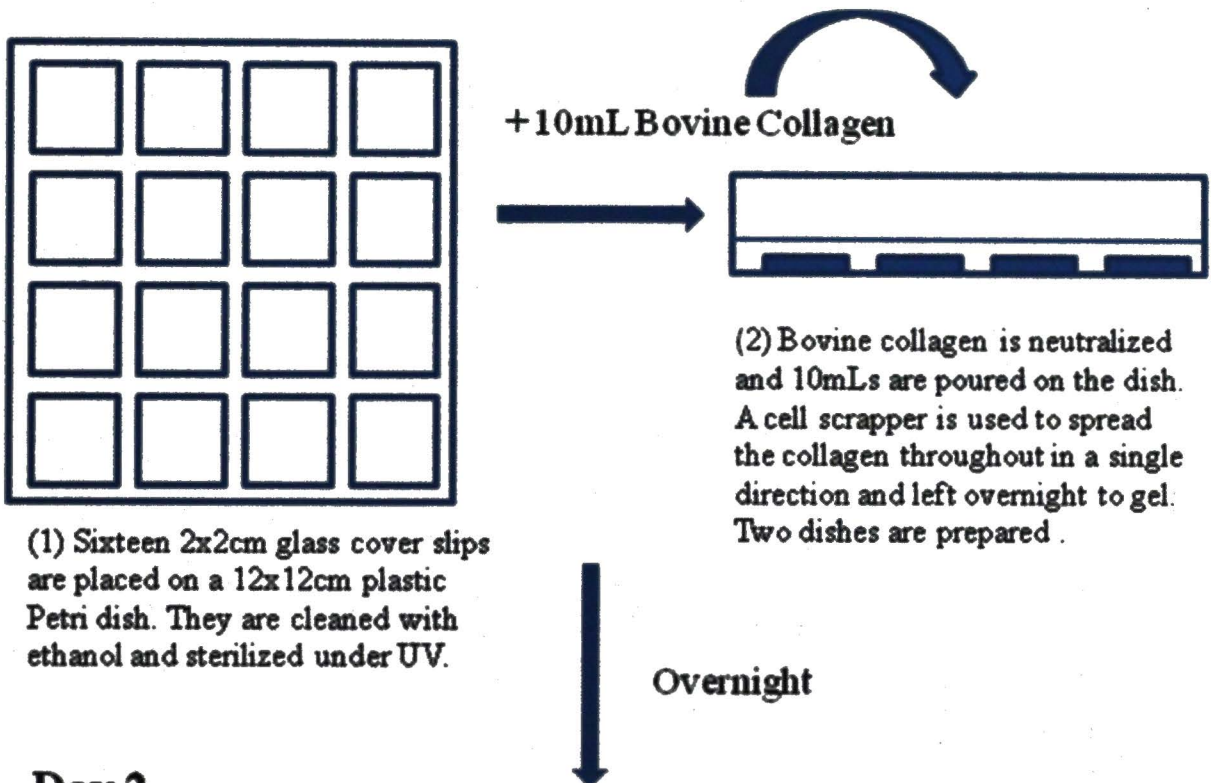
(c) Spectrum of CMTMR (Cell Tracker Orange®)

(c)

Absorption

Fluorescence emission

400   450   500   550   600   650   700
Wavelength (nm)
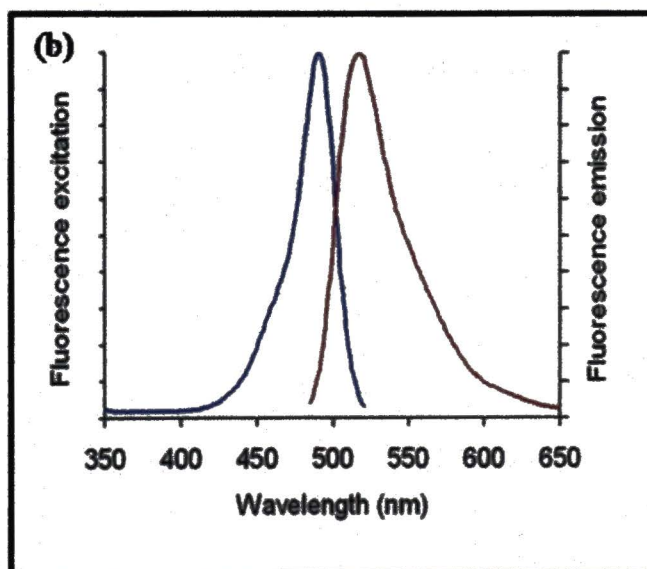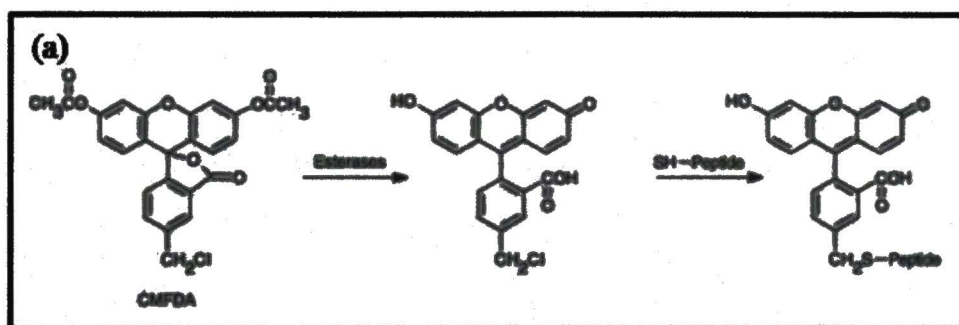
Figure 3.2: schematic representation of the corneal stroma collagen film stack protocol.

Day 1

+10mL Bovine Collagen

(2) Bovine collagen is neutralized and 10mLs are poured on the dish. A cell scrapper is used to spread the collagen throughout in a single direction and left overnight to gel. Two dishes are prepared.

(1) Sixteen 2x2cm glass cover slips are placed on a 12x12cm plastic Petri dish. They are cleaned with ethanol and sterilized under UV.

Overnight

Day 2

Petri dish 1 seeded with fibroblasts labeled with Red Cell Tracker®

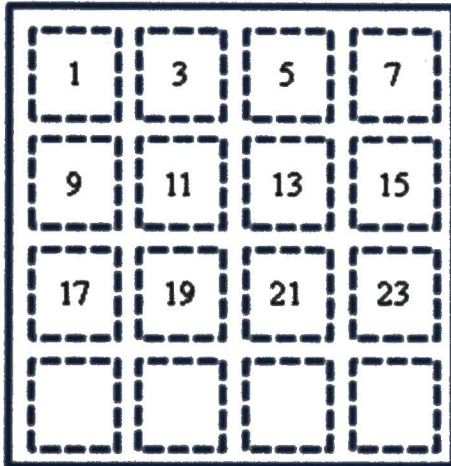Petri dish 2 seeded with fibroblasts labeled with Green Cell Tracker®

(3) Stromal fibroblasts are labeled with either Orange or Green Cell Tracker® on Day 1, harvested, and plated on collagen film on Day 2.
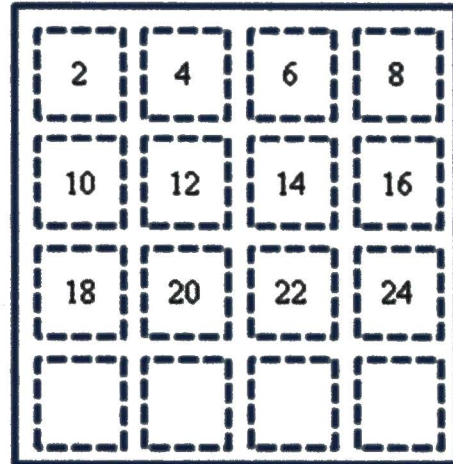(4) 1.0×10^5 cells are seeded on each cover slip and allowed to attach overnight.
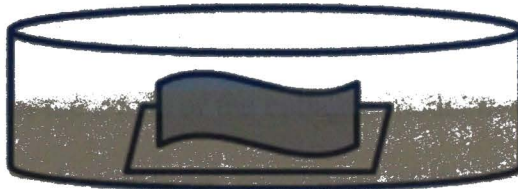
Day 3

Petri Dish 1

1	3	5	7
9	11	13	15
17	19	21	23

Petri Dish 2

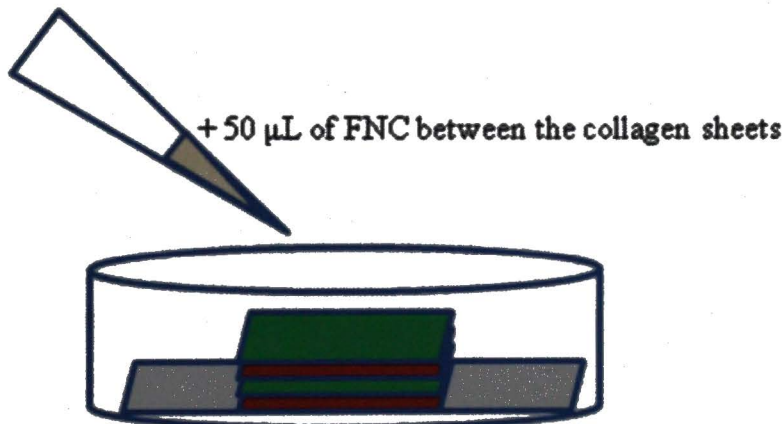| 2	4	6	8
10	12	14	16
18	20	22	24

(5) The collagen around each cover slip is carefully cut using a scalpel.

(6) The cut collagen is lifted from the Petri dish with the cover slip and placed in a circular Petri dish full of HAMS F12 media to allow the collagen sheet to peel off gently from the glass cover slip.

+ 50 µL of FNC between the collagen sheets

(7) The collagen sheet is then lifted using forceps to hold two corners and carefully placed on a collagen sponge to provide the stack with ample nutrients. Fibronectin (FNC) is used as an adhesive between the sheets to "glue" the stack together.

RESULTS

Corneal stroma constructs

The collagen sheets were prepared as previously described and seeded with fluorescently labeled green and orange cells (Figure 3.3). The methodology was tested for 10 film stacks first (figure 3.4), and then for 20 film stacks (Figure 3.5) and examined using confocal microscopy. Images of x-y and z scans were obtained and were captured every 20μm in the 10 film stack, and every 25μm in the 20 film stack. The complete galleries of z-scan images for each collagen film stack were compiled into a single 3-dimensional projection to demonstrate the alternating green and red fluorescence of the stacked models (Figure 3.6). The results show successful alternation of the green and orange-labeled cells across the z-axis of the collagen model in which alternating films are uniformly distanced apart. A significant percentage of the films were also successfully aligned orthogonally to one another, this is shown in figure 3.6 (a) and (b) where the films carrying the orange labeled cells are thicker (the cells are sectioned laterally on the x-y plane), than the films carrying the green labeled cells (the cells are coming out of the x-y plane). Notice that in the 10 film stack only 9 layers are visualized, and in the 20 film stack only 16 layers are visualized, suggesting that the cells on the missing films did not survive in the compressed collagen stack.

Corneal stromal construct cross sections

After image acquisition of the 10 film collagen stack was complete, the construct was paraffin embedded as previously described and sectioned (~7μm); then viewed by confocal microscopy as shown in Figure 3.7. These results show the analogous succession of collagen films carrying green and orange cells as seen in figure 3.6. This was then compared to indirect immunofluorescence of human cornea donor sections prepared as described previously in Figure 3.8. The results show analogy and similarity in structure and cell distribution and alignment between the cross section of the collagen stack (figure 3.7) and the corneal stroma cross section (figure 3.8), suggesting that the collagen stack model is structurally homologous to that of the corneal stroma.

Cytoskeletal protein expression in corneal stromal fibroblasts

A comparison between corneal stromal fibroblasts seeded on glass and thin collagen sheets using indirect fluorescence demonstrated the differences in morphology and cytoskeletal protein expression of MHC (Figures 3.9 through 3.11), MLC (Figures 3.12 through 3.14), α-SMA (Figures 3.15 though 3.17) and Vim (Figures 3.18 though 3.20). These results show that the extended morphology of the corneal stromal fibroblasts seeded on thin collagen sheets are very similar to the morphology of the corneal stromal fibroblasts in the human corneal stroma tissue seen in figure 3.8. They show extended fibers of the cytoskeletal proteins: α-SMA, MHC, MLC, and Vim. The cells on the thin collagen sheets are also aligned in a parallel arrangement similar to that seen on the human corneal stroma tissue. On the other hand, the corneal stromal fibroblasts seeded on

49

the glass cover slips (Figures 3.9 through 3.20 (c) and (d) show a very different morphology to that seen on the thin collagen sheets (figures 3.9 through 3.20 (a) and (b)), and the human corneal stroma tissue. The morphology of the cells on the glass cover slips are of irregular size and have flat morphology, even though the expression of the cytoskeletal proteins are not very different to that seen of the cells seeded on the thin collagen sheets, they do not correspond to the visible extended fibers of the cytoskeletal proteins as do the cells on the thin collagen sheets. The expression of MLC in the corneal stromal fibroblasts seeded on the thin collagen sheets (Figure 3.12 through 3.14 (a) and (b)) is concentrated in the nuclear region as seen in the cells in the human corneal stroma tissue, however this is different from the expression of MLC in the corneal stromal fibroblasts seeded on glass cover slips which is expressed on the entire surface area of the cell as seen in figures 3.12 through 3.14 (c) and (d).

Optical properties of the corneal stroma construct

The percentage transmissions of two stacks composed of 20 thin films of collagen were measured using a spectrophotometer (Figure 3.21). The first collagen stack was sandwiched between two collagen sponges to keep the sample well hydrated with media, in the process the construct was compressed and became thinner (~1mm) (Figure 3.21 (a)). This sample showed a percentage transmission of 50% at a wavelength of 700nm. The second sample that was not sandwiched between two collagen sponges remained the same original thickness (1.6mm) and showed a percentage transmission of 40% at a wavelength of 700nm (Figure 3.21 (b)).

The transparencies of the two samples were then further investigated by placing them on typed text, and determine the visibility of the letters through the collagen stacks. The letters that were under the thin, "compressed" collagen stack (Figure 3.22 (a) and (c)) were more visible than the letter under the thicker, "uncompressed" collagen stack (Figure 3.22 (b)).

The optical activity of the collagen stack was demonstrated by testing its polarization properties (Figure 3.23 & 3.24). The stack was placed between two polarizers. The first one was mounted on the light source, the stack was placed on top of the first polarizer, then the second polarizer was rotated (a) $0°$, (b) $60°$, (c) $90°$, (d) $120°$, and (e) $180°$ from the first polarizer (Figure 3.23 & 3.24). When the second polarizer was $0°$ and $180°$ with respect to the first polarizer (on the same principal axis), the light passing through the collagen stack was depolarized as seen in figure 3.24 (a) and (e), but became completely polarized when the second polarizer was $90°$ (perpendicular to the principal axis) with respect to the first polarizer as seen in figure 3.24 (c).

Figure 3.3: Confocal images of corneal stromal fibroblasts seeded on thin collagen sheets labeled with Cell Tracker Green® (a) & (b), and Cell Tracker Orange® (c) & (d).
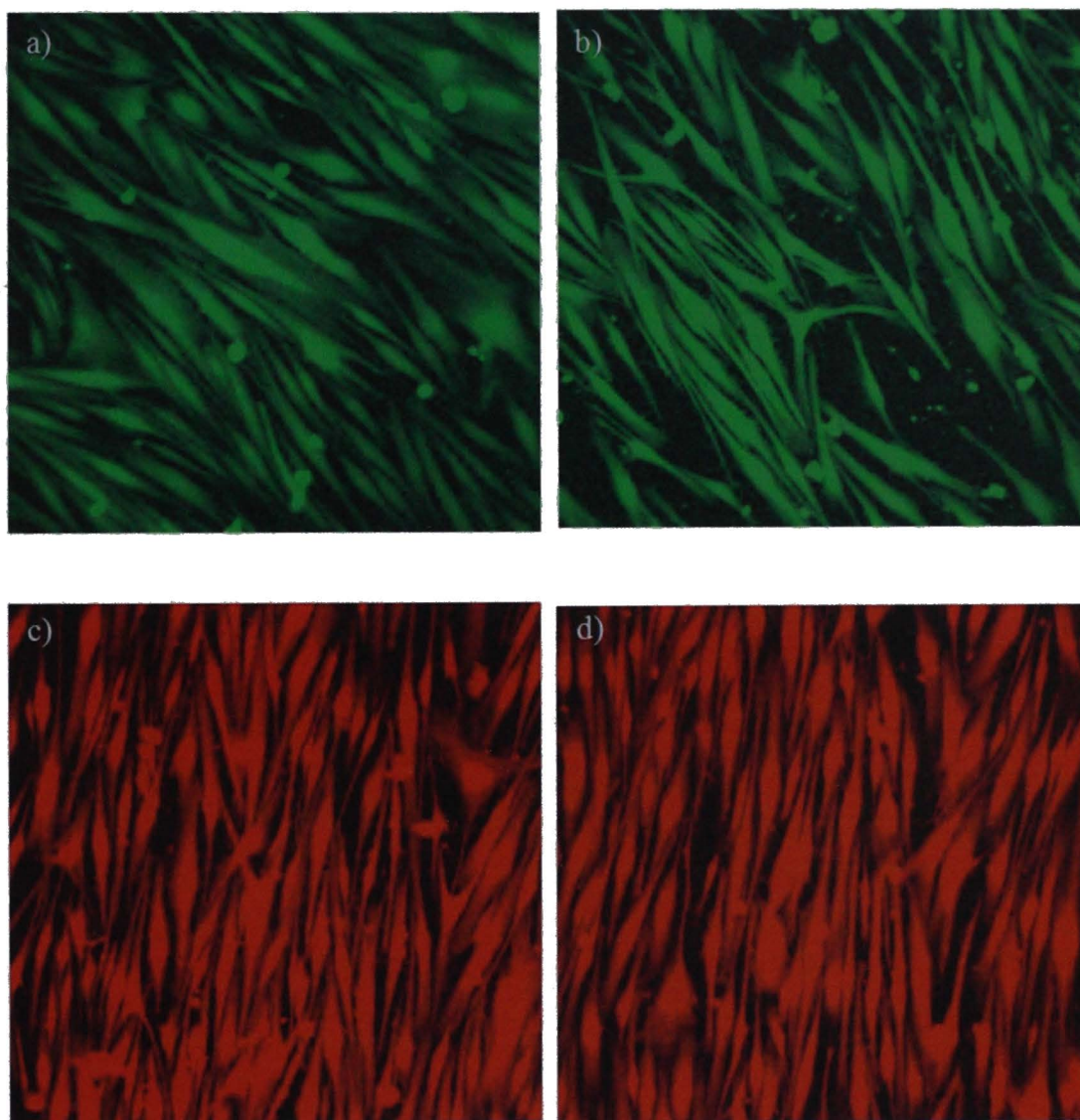
Figure 3.4: A scan of confocal images through the z-axis of a 10 film stack of collagen and alternating labeled cells of red and green. Images were captured every 25μm.
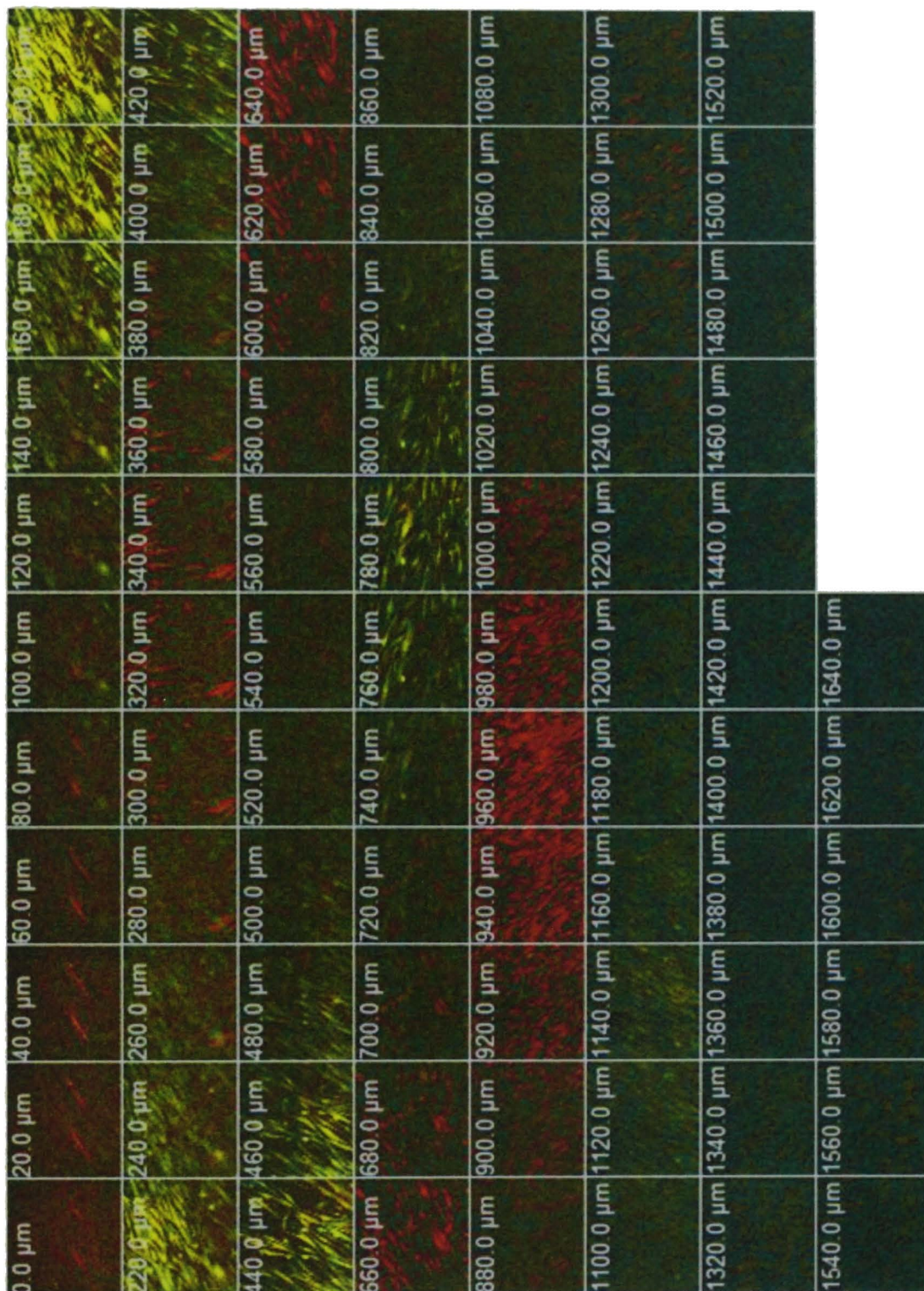
Figure 3.5: A scan of confocal images through the z-axis of a 20 film stack of collagen and alternating labeled cells of red and green. Images were captured every 25µm.

Figure 3.6: A 3-Dimensional projection compiled the series of confocal images through the z-axis of the 10 layer stack (a), and the 20 layer stack (b).
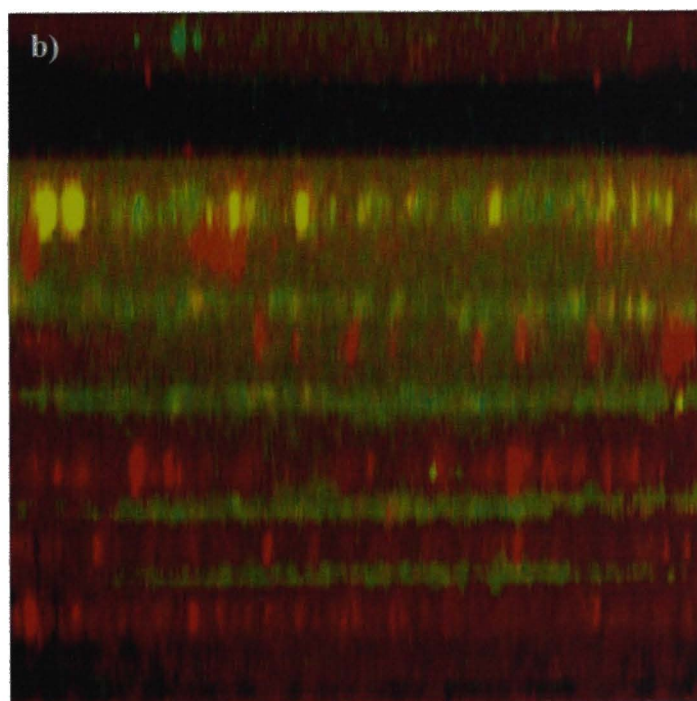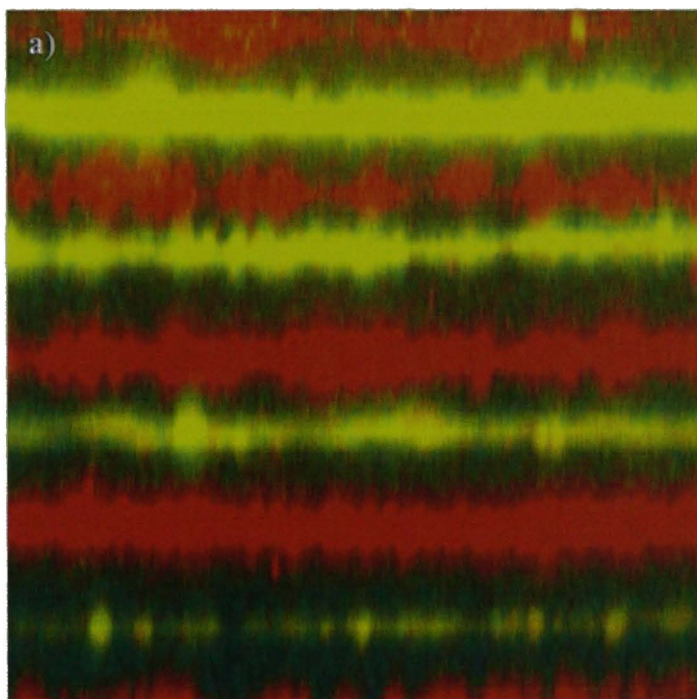
Figure 3.7: The 10 layer stack cornea construct was prepared for paraffin sections and looked under the confocal microscope (a) & (b).
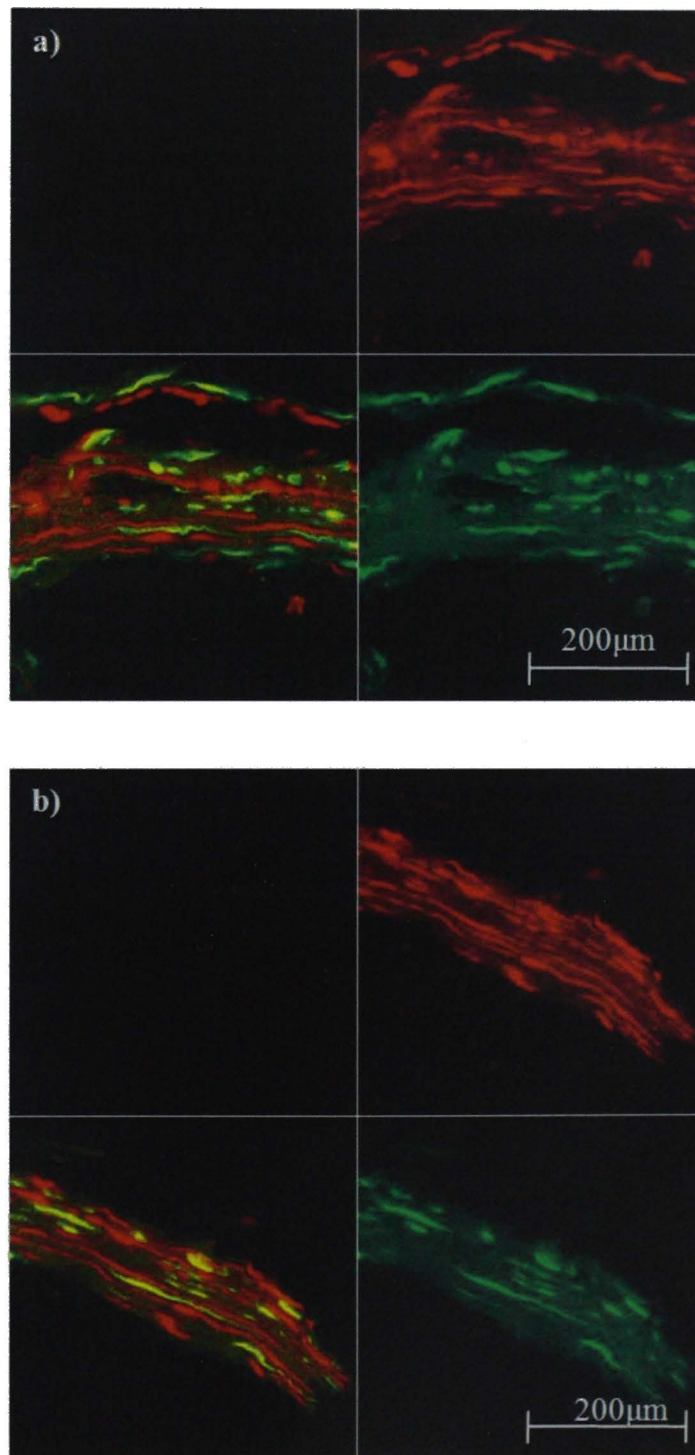
Figure 3.8: Human donor cornea sections in 20x magnification demonstrating the expression of MHC (a), and Vimentin (b).

Figure 3.9: Expression of Myosin Heavy Chain (MHC) in stromal fibroblasts seeded on thin sheets of collagen (a) & (b), and glass (c) & (d) on 4x magnification epifluorescence.
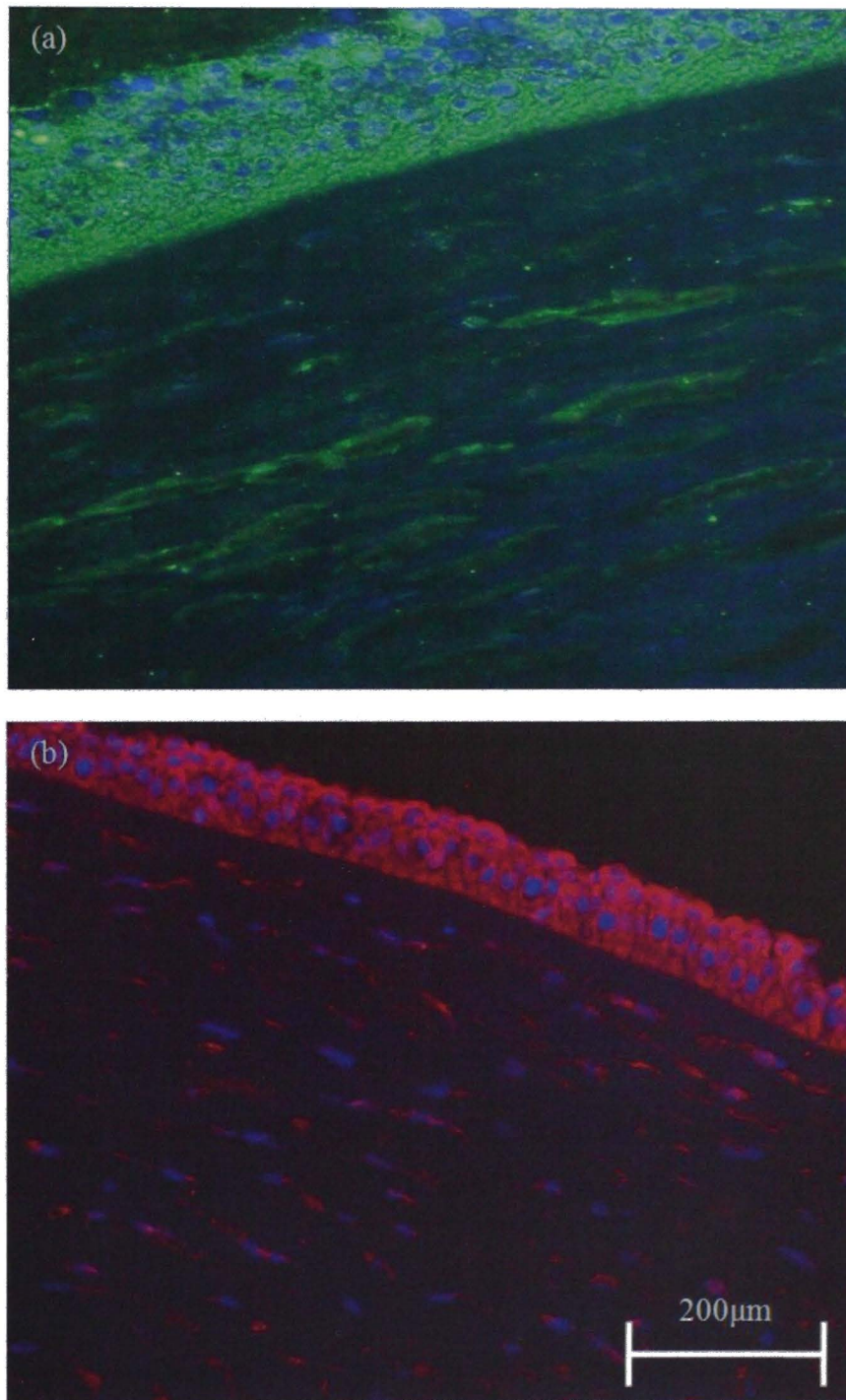
Figure 3.10: Expression of Myosin Heavy Chain (MHC) in stromal fibroblasts seeded on thin sheets of collagen (a) & (b), and glass (c) & (d) on 10x magnification epifluorescence.

Figure 3.11: Expression of Myosin Heavy Chain (MHC) in stromal fibroblasts seeded on thin sheets of collagen (a) & (b), and glass (c) & (d) on 20x magnification epifluorescence.

Figure 3.12: Expression of Myosin Light Chain (MLC) in stromal fibroblasts seeded on thin sheets of collagen (a) & (b), and glass (c) & (d) on 4x magnification epifluorescence.

Figure 3.13: Expression of Myosin Light Chain (MLC) in stromal fibroblasts seeded on thin sheets of collagen (a) & (b), and glass (c) & (d) on 10x magnification epifluorescence.
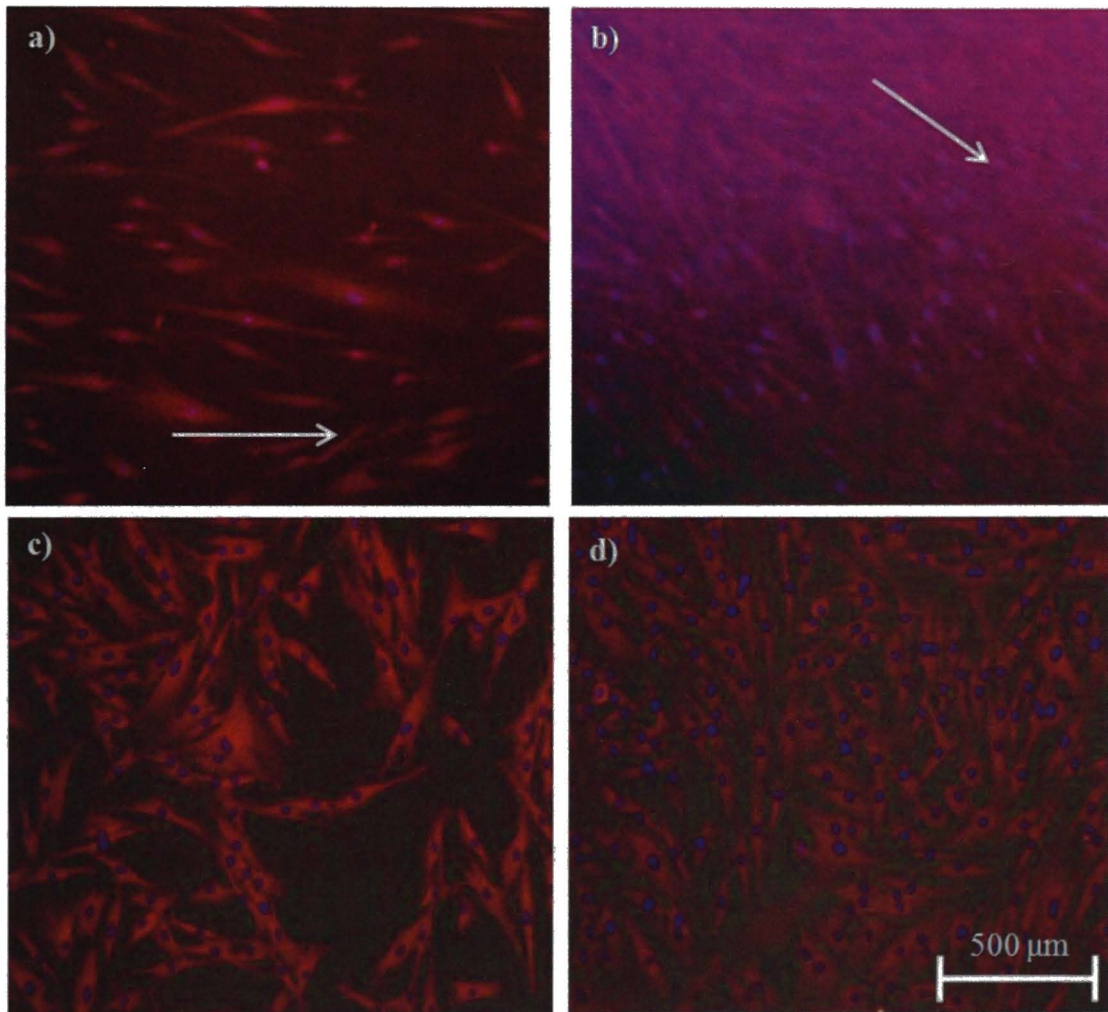
Figure 3.14: Expression of Myosin Light Chain (MLC) in stromal fibroblasts seeded on thin sheets of collagen (a) & (b), and glass (c) & (d) on 20x magnification epifluorescence.
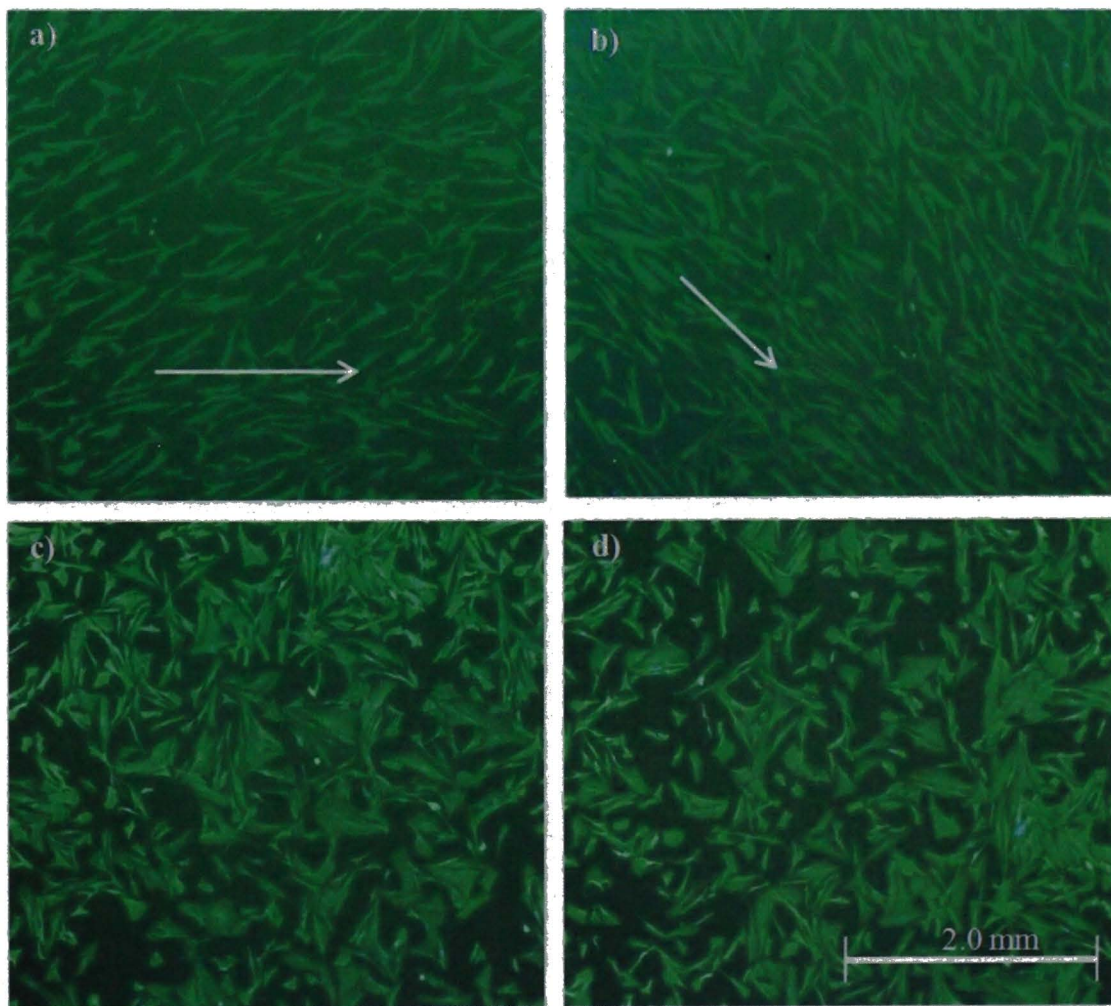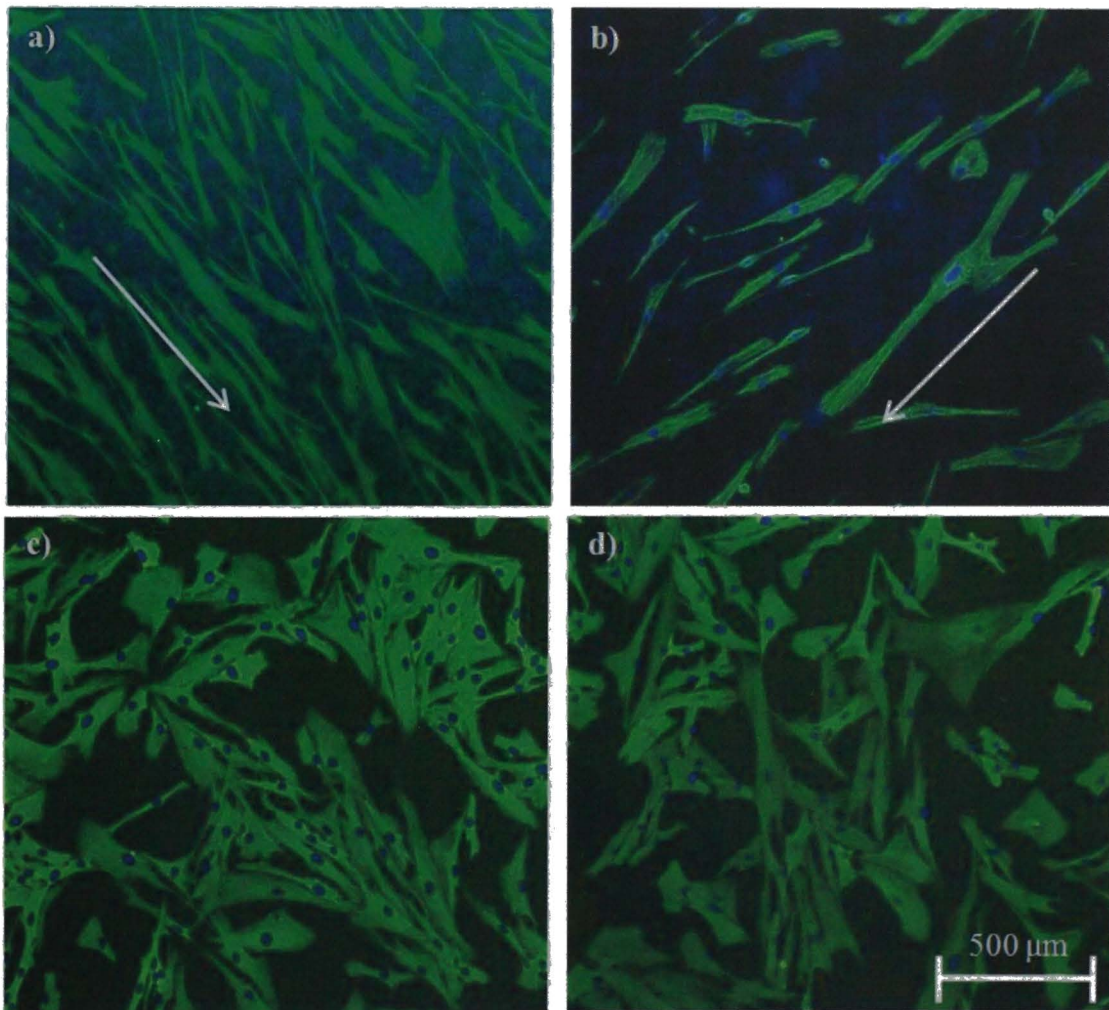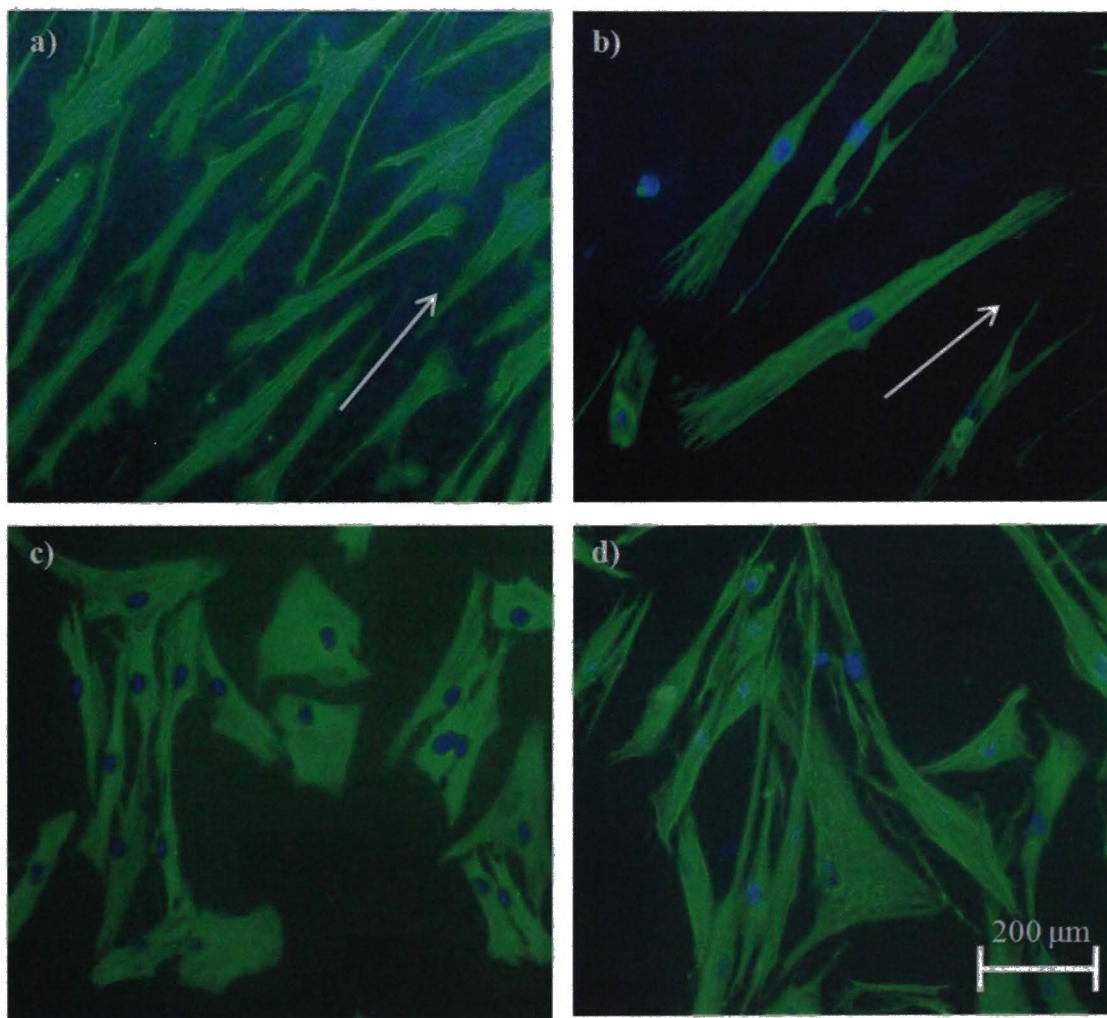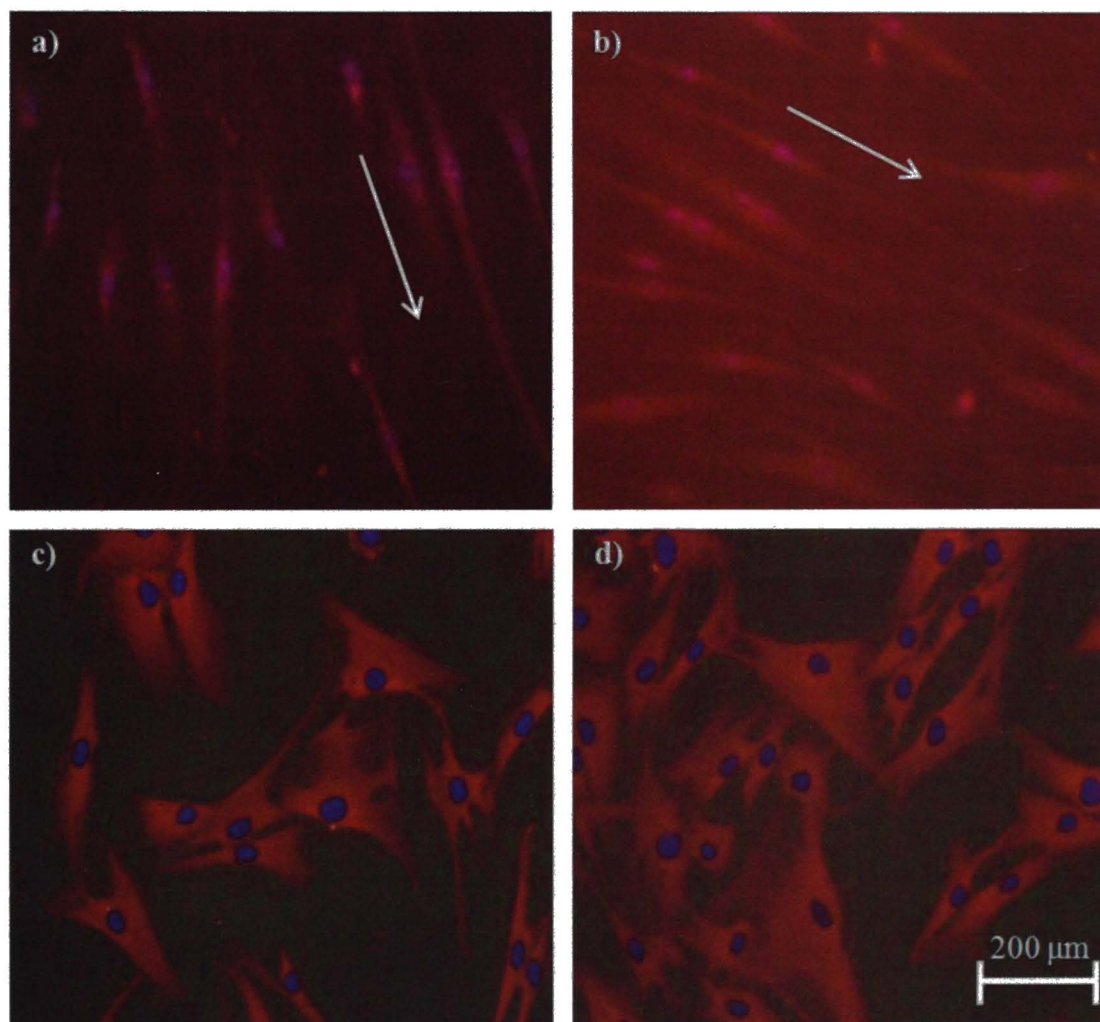
Figure 3.15: Expression of Smooth Muscle Actin (SMA) in stromal fibroblasts seeded on thin sheets of collagen (a) & (b), and glass (c) & (d) on 4x magnification epifluorescence.
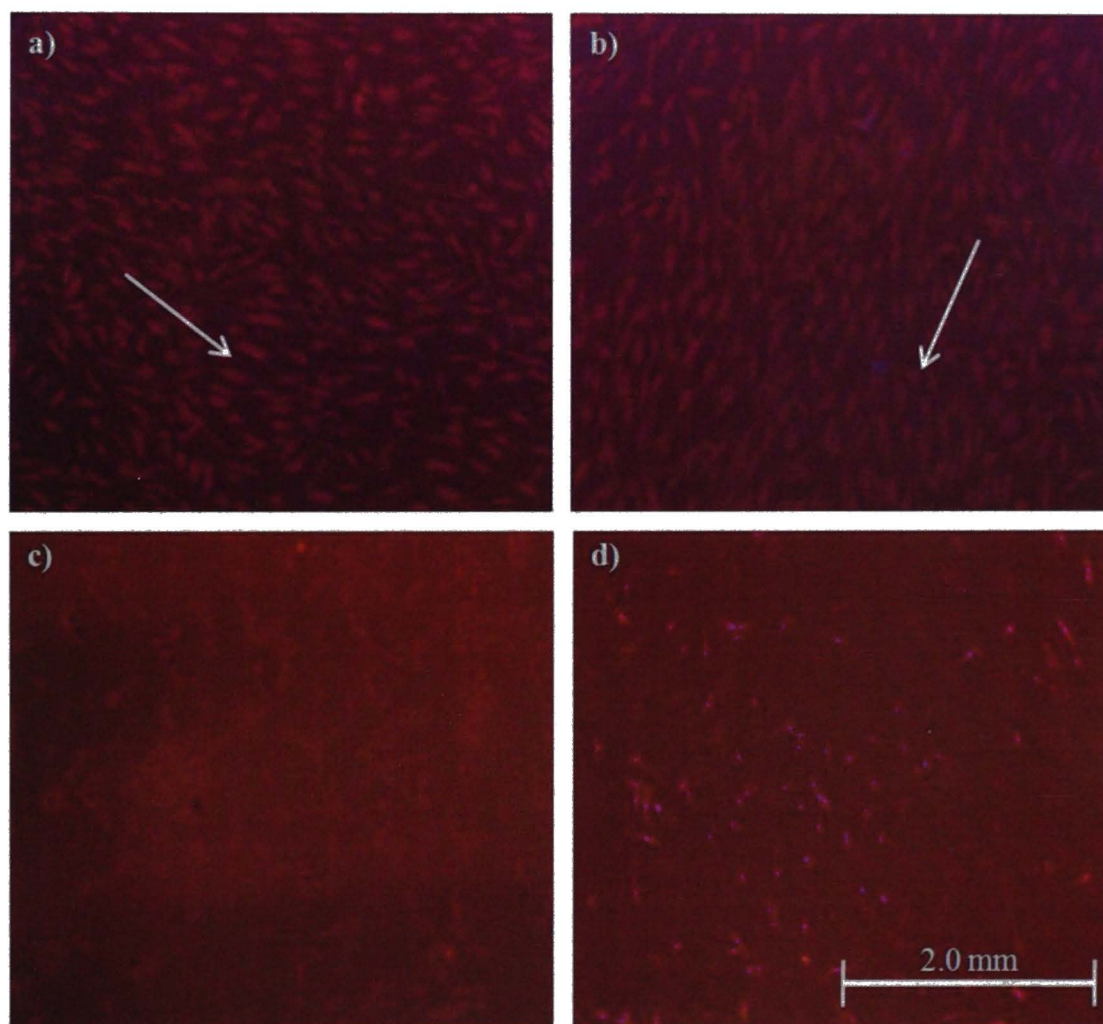
Figure 3.16: Expression of Smooth Muscle Actin (SMA) in stromal fibroblasts seeded on thin sheets of collagen (a) & (b), and glass (c) & (d) on 10x magnification epifluorescence.
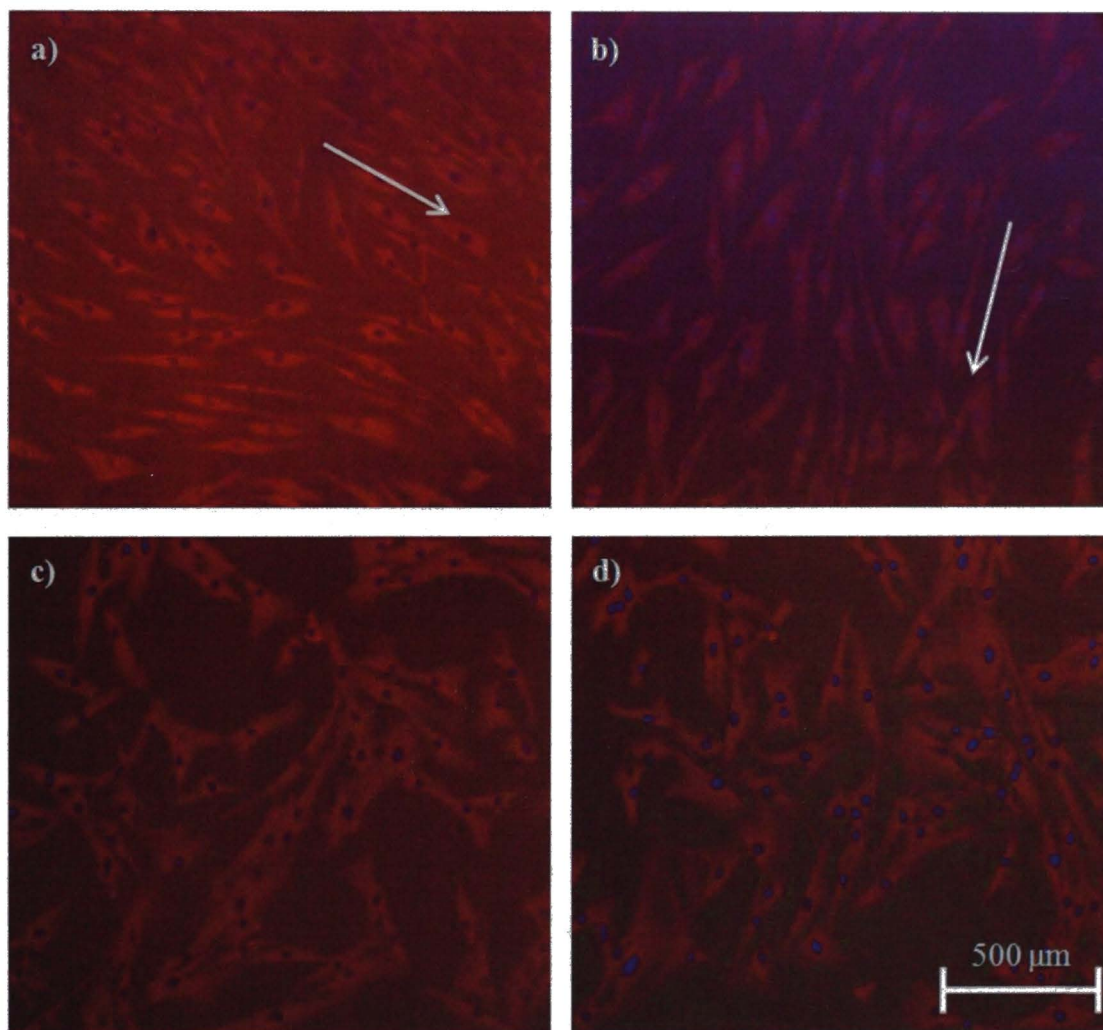
Figure 3.17: Expression of Smooth Muscle Actin (SMA) in stromal fibroblasts seeded on thin sheets of collagen (a) & (b), and glass (c) & (d) on 20x magnification epifluorescence.
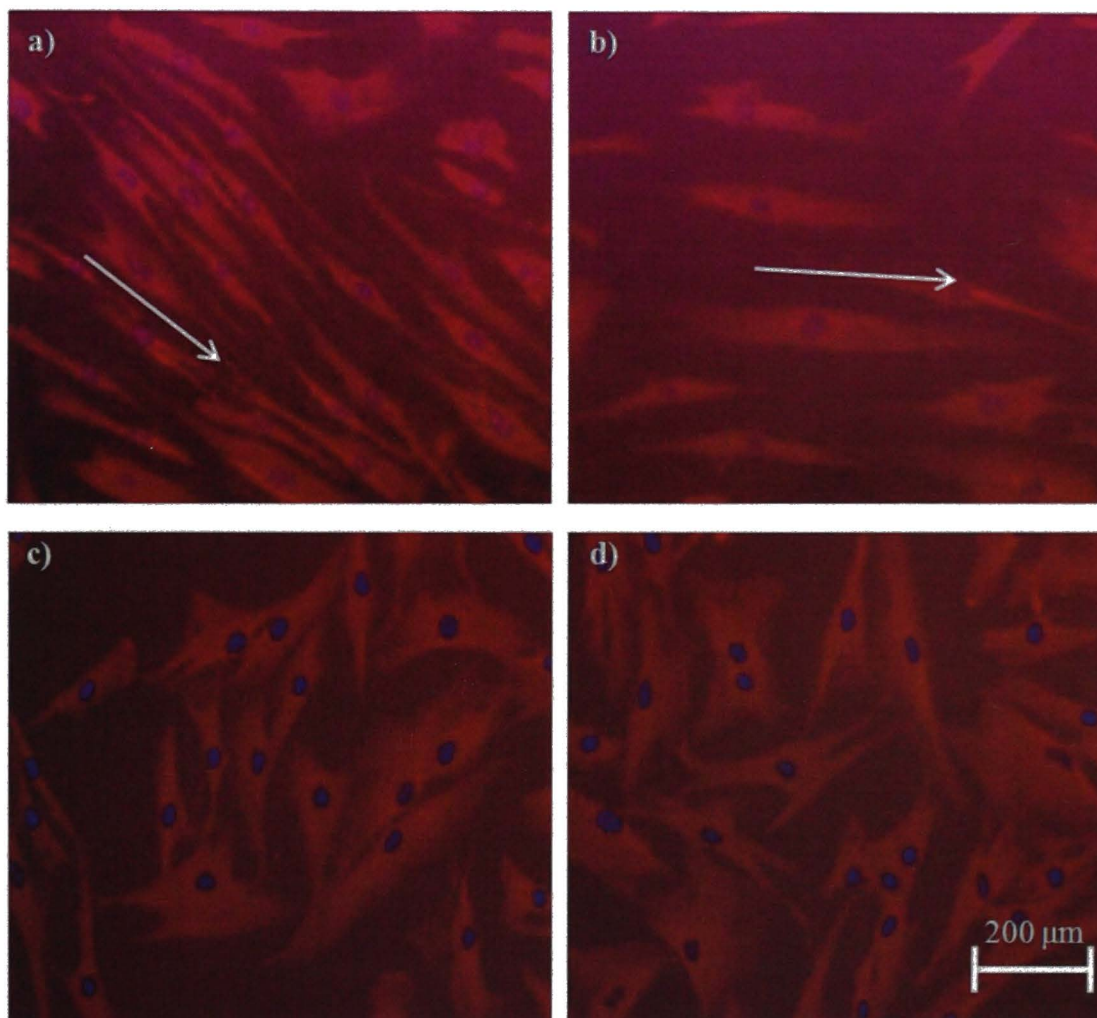
Figure 3.18: Expression of Vimentin (Vim) in stromal fibroblasts seeded on thin sheets of collagen (a) & (b), and glass (c) & (d) on 4x magnification epifluorescence.
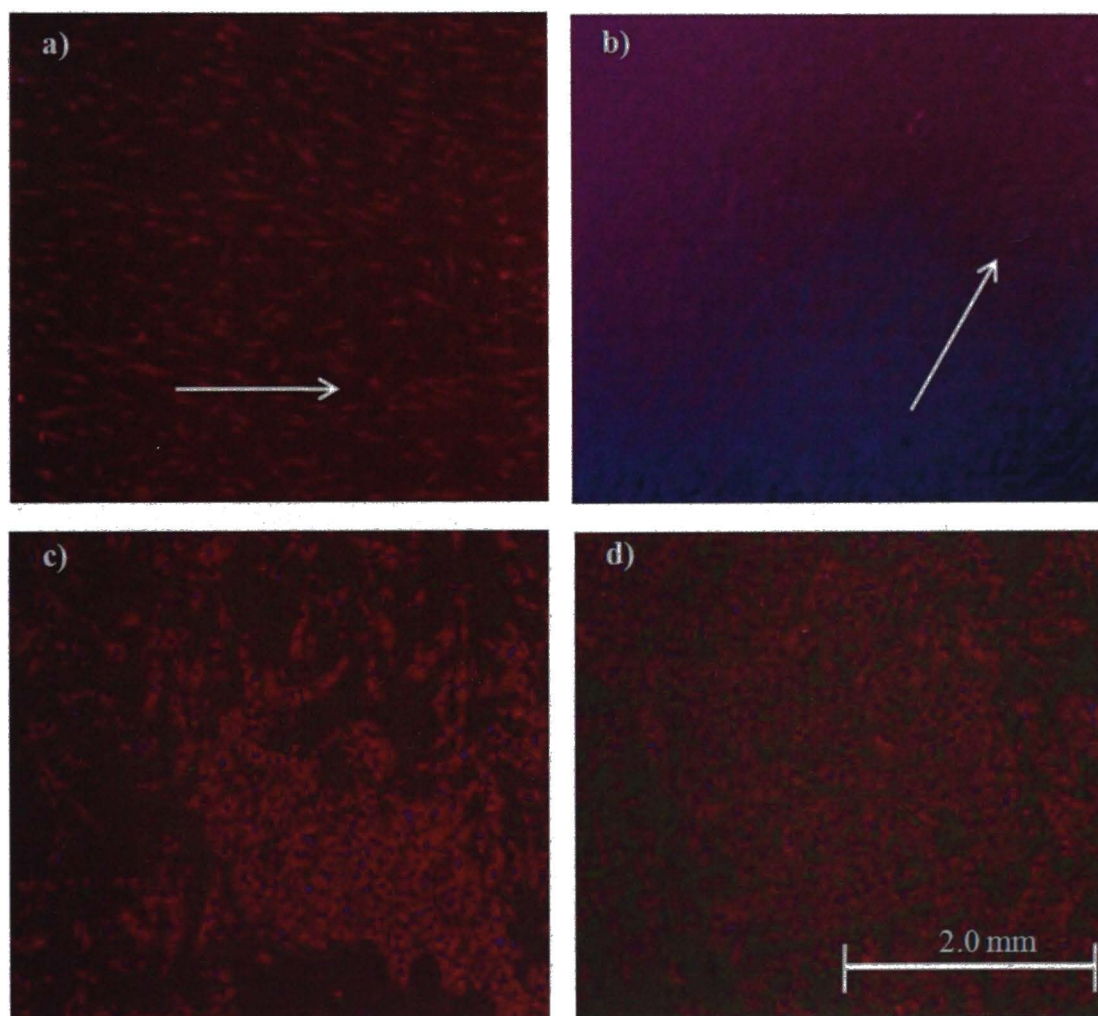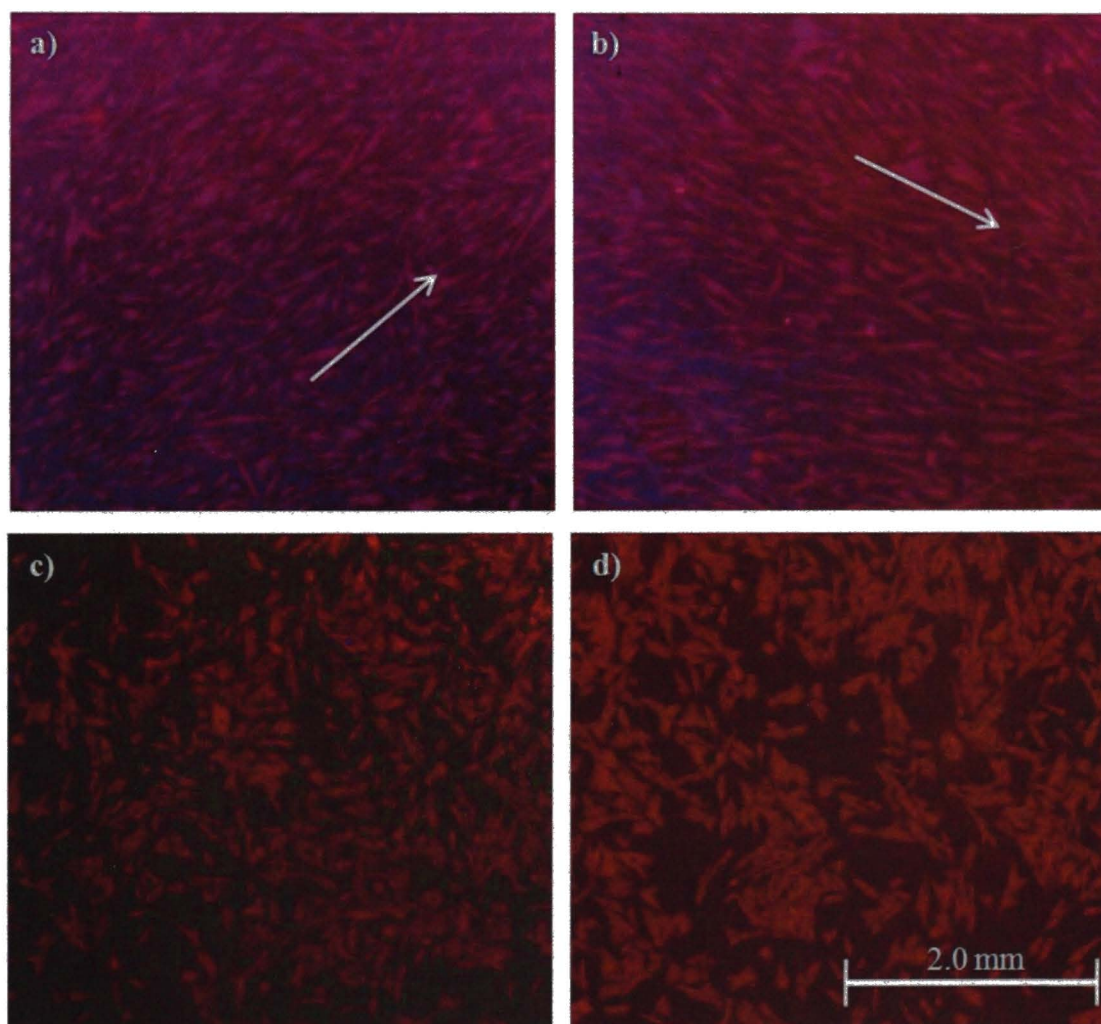
Figure 3.19: Expression of Vimentin (Vim) in stromal fibroblasts seeded on thin sheets of collagen (a) & (b), and glass (c) & (d) on 10x magnification epifluorescence.
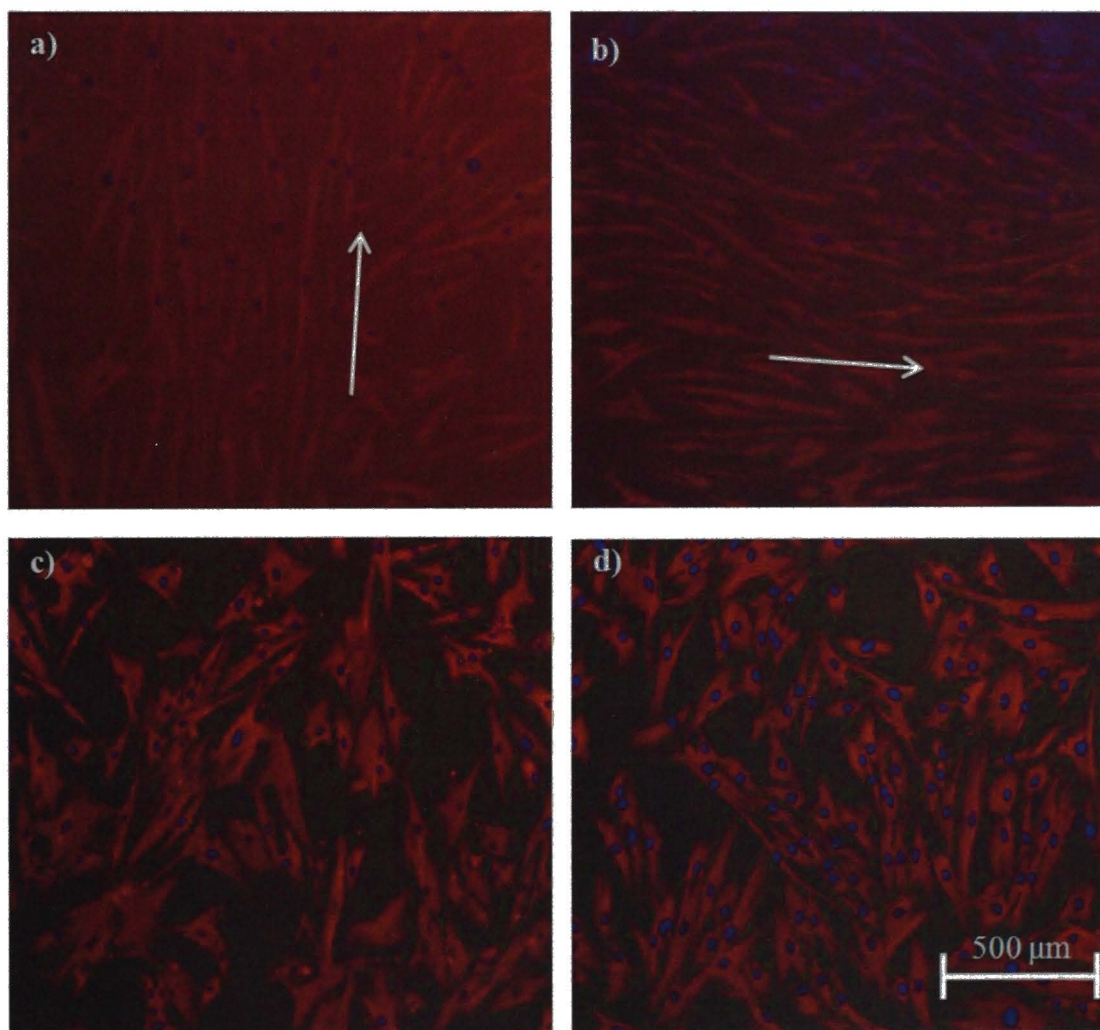
Figure 3.20: Expression of Vimentin (Vim) in stromal fibroblasts seeded on thin sheets of collagen (a) & (b), and glass (c) & (d) on 20x magnification epifluorescence.
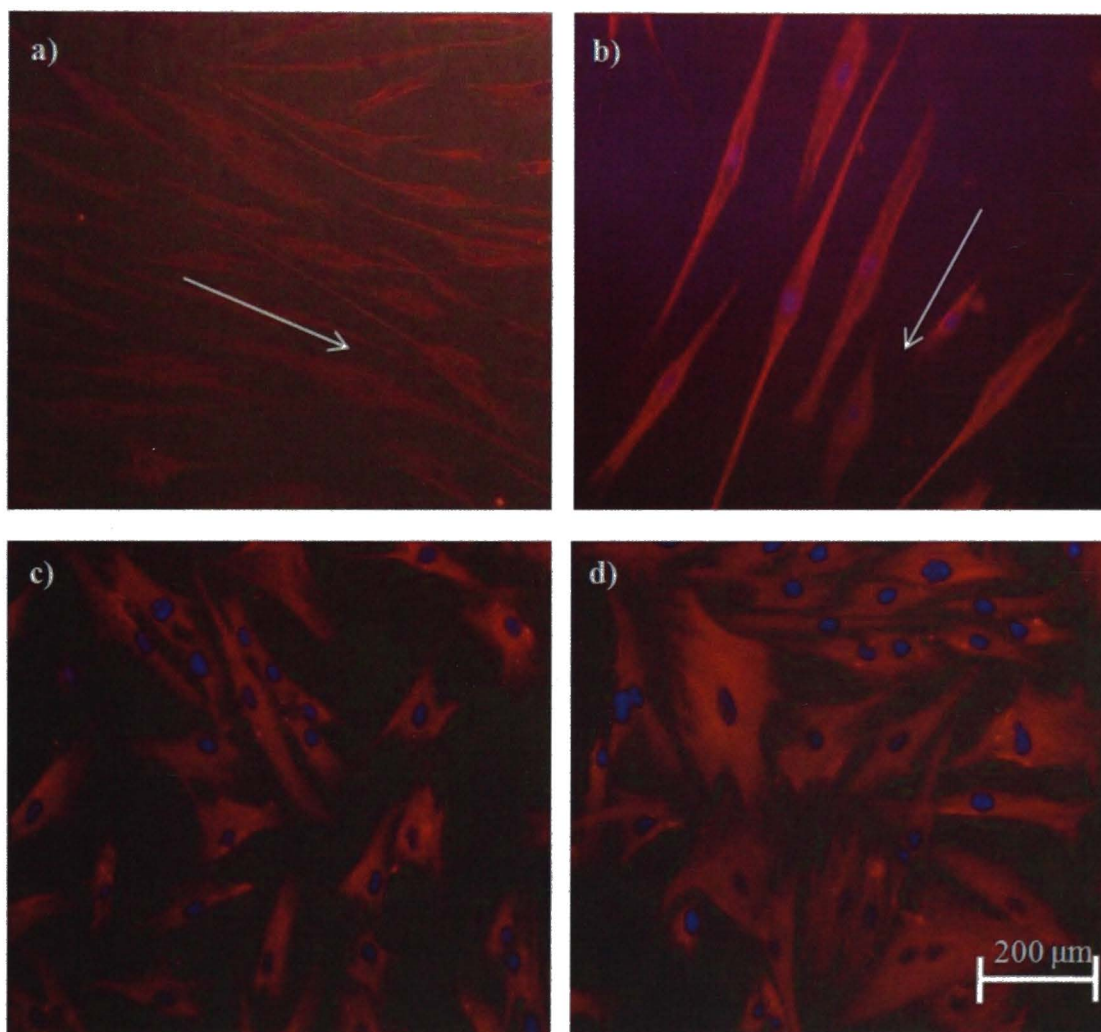
Figure 3.21: Percentage transmission of two 20 layer collagen stacks: one was sandwiched between to collagen sponges to make it thinner (a), and the other was not (b).

(a) Continuous line

(b) Dashed line
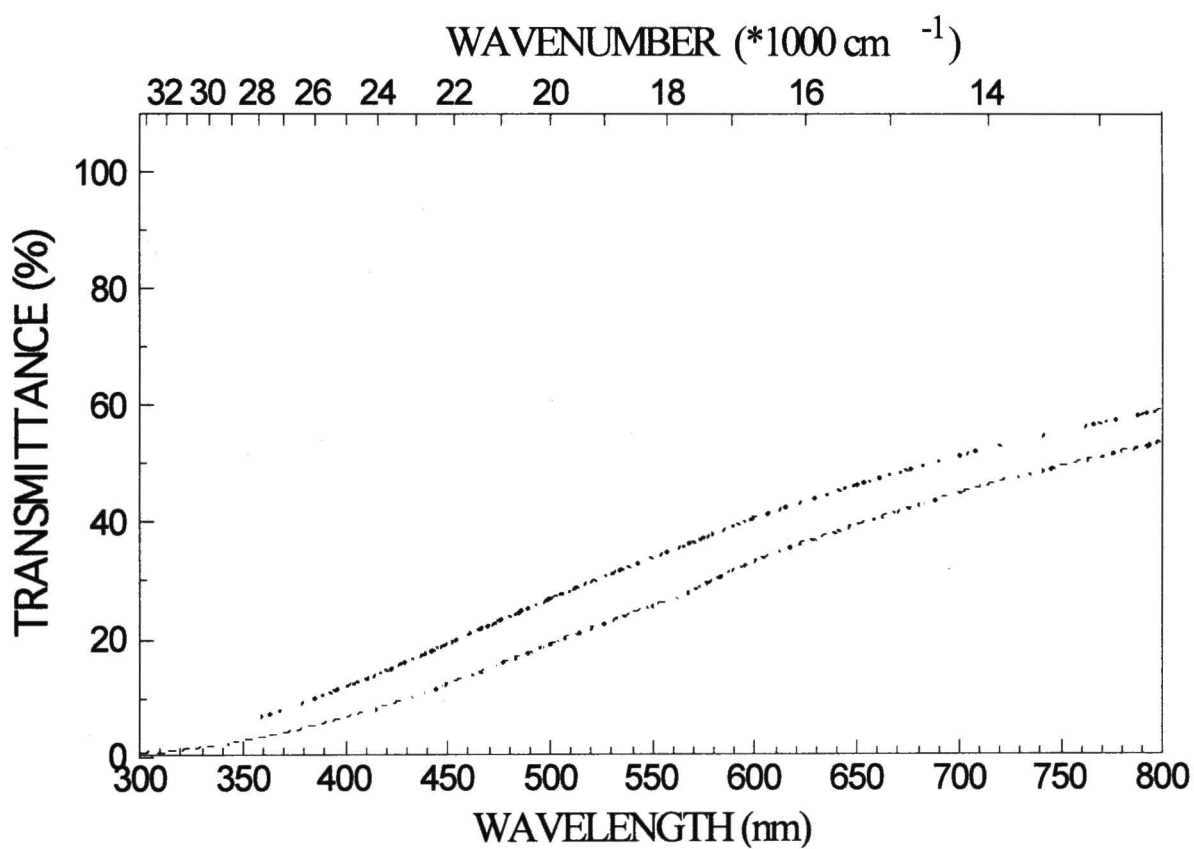
Figure 3.22: A photograph to test the transparency of the 20 layer stack collagen construct that was sandwiched between two collagen sponges to make it thinner (a) & (c), and (b) which was not, by placing it on typed text.
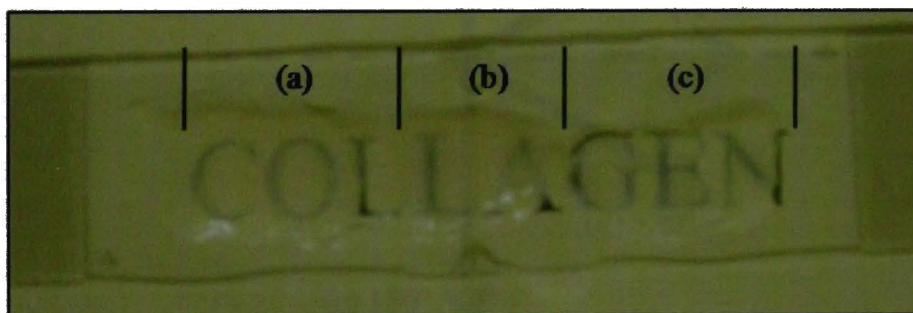
Figure 3.23: A schematic illustrating the orientation of the two polarizers in reference to the principal axis.
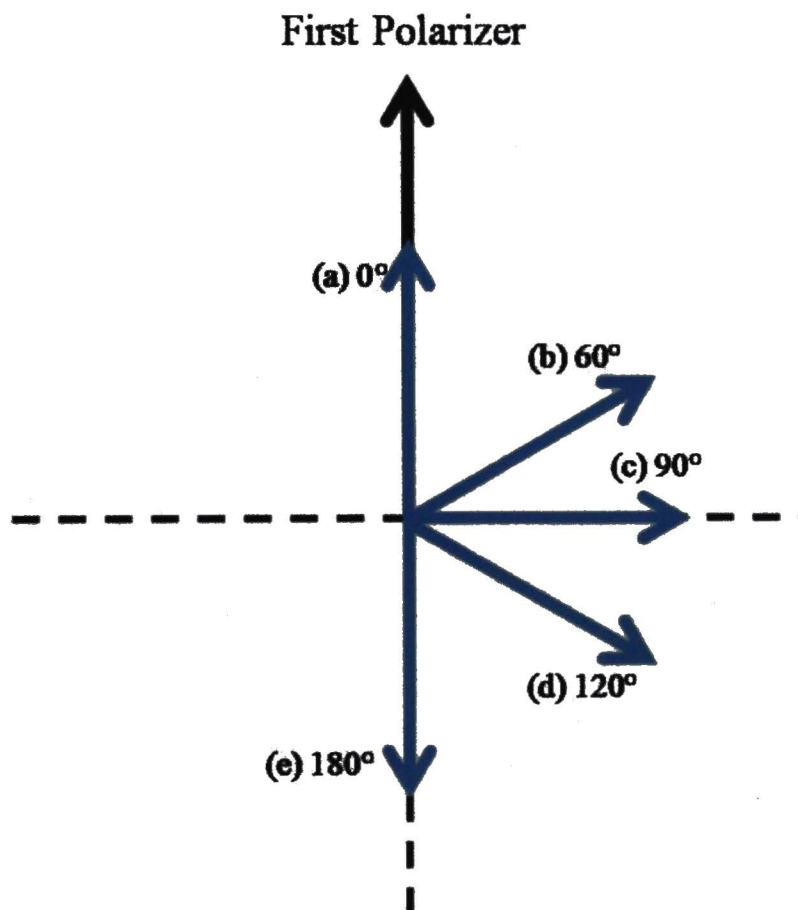
Figure 3.24: Photographs of the collagen stack when the second polarizer is at (a) 0°, (b) 60°, (c) 90°, (d) 120°, and (e) 180° from the first polarizer.
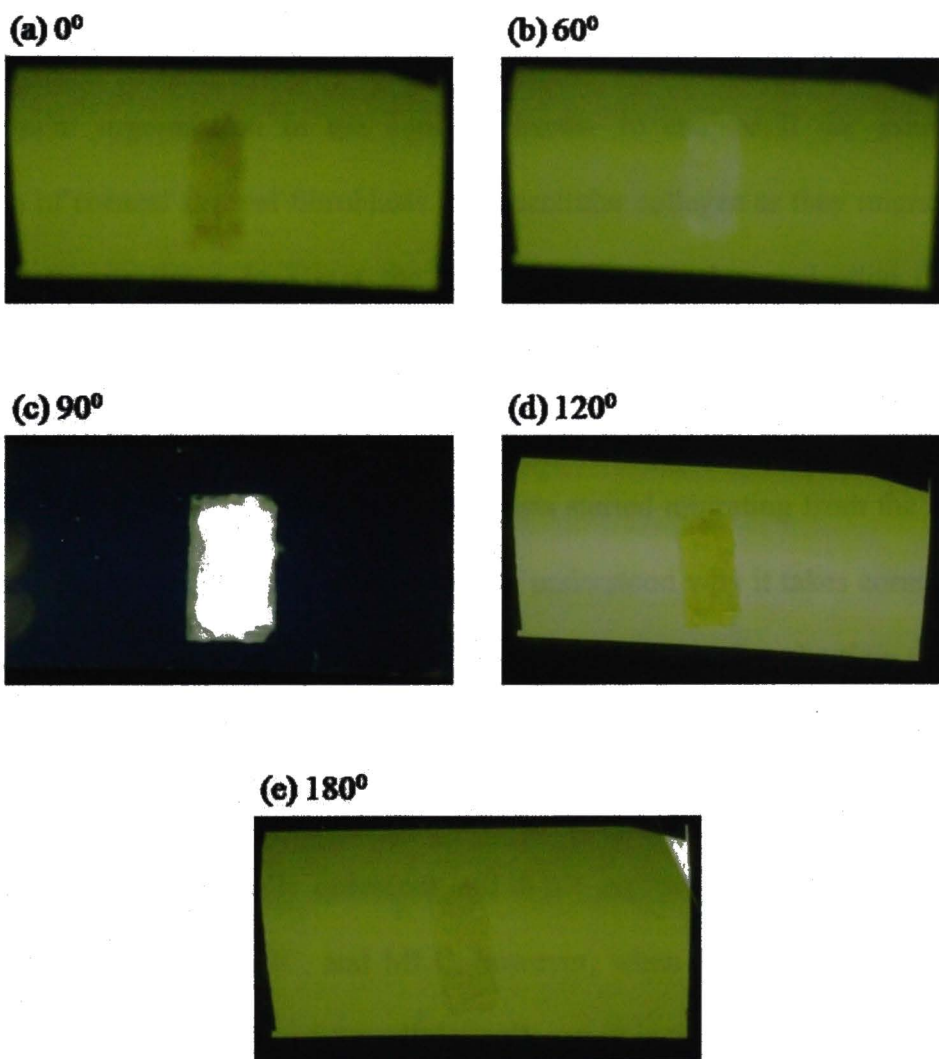
CHAPTER IV

DISCUSSION AND CONCLUSION

The purpose of this study was to test the hypothesis that collagen organization directs cellular organization in the corneal stroma. In chapter II we examined the distribution of corneal stromal fibroblasts in an acellular collagen as they migrated out of the corneal stroma tissue to assess the role of collagen gel organization on cellular arrangement *in vitro*. Corneal stromal biopsies as shown in figure 2.1 (a) were implanted in acellular bovine collagen type I gel and were observed under phase contrast microscopy. At day 10, corneal stromal fibroblasts started migrating from the tissue into the surrounding matrix. It is still not completely understood why it takes corneal stromal fibroblasts 10 days to begin migrating into the acellular matrix, but the time seems to be reproducible. We hypothesize that this might be a consequence of corneal stromal fibroblasts' activation and response to wound healing stimulation. Corneal stromal fibroblasts in tissue are usually quiescent and don't express high levels of cytoskeletal proteins such as α-SMA, MHC, and MLC, however, when the corneal stroma biopsies are dissected and immersed into the acellular collagen, it is thought that the 10 days is the time it takes corneal stromal fibroblasts to become activated to the now "injured stroma" and start migration as they would in a wounded stroma. This is considered to be an excellent model to study wound healing processes *in vitro*. A number of punch biopsies may be obtained from a pair of human donor corneal stromas as shown in figure 2.1 (a).

Figures 2.1 (c) and (d) show the corneal stromal fibroblasts migrate in a random fashion into the surrounding acellular collagen gel. The acellular collagen gel is not an organized matrix and has less densely packed collagen fibers than the corneal stroma tissue as shown in the hematoxylin and eosin stained cross section in figure 2.1 (b). As a result, it can be concluded that the orientation and alignment of corneal stromal fibroblasts *in vivo* is consequence of the ECM organization in the corneal stroma. The collagen fibrils are aligned in parallel and are linked together through lamellar cross-links at fixed lamellar distances. This structure controls the spatial arrangement of the corneal stromal fibroblasts, which in turn cause the synthesis and production of collagen fibers that will maintain this alignment.

As a result, the next step was to examine the feasibility of constructing a model that will mimic the lamellar organization of collagen and thus direct cellular organization in the corneal stroma. Several methodologies were tested to successfully stack collagen films in an efficient, feasible and reproducible protocol. Initially, the collagen films were poured separately in 6-well plates, and each film composed of 0.5mLs of collagen; after fibrillogenesis, cells were seeded on top of the film, and allowed to attach overnight and stretch before the next film of collagen layer is cast on top. This methodology took six weeks to produce 8 film stacks of collagen and cells; the films were too thick and were continuously contracting as the stack increased due to the fetal bovine serum (FBS) in the culture media. It was very challenging to keep the cells on the bottom films viable since access of the culture media to the cells through the thick films was impaired. Also, the

cells were attached randomly on the collagen film and several mechanical manipulations were investigated to try to align the cells on the films with very little success (silk threads, plastic and metal imprinted grooves). However, through numerous trial-and-error methodologies formulated after that, we finally succeeded in designing the protocol described in figure 3.2. This protocol allowed the construction of up to 16 very thin collagen films (~100μm) per Petri dish (two Petri dishes were used; one for each color of fluorescently labeled cells), and more efficient cell seeding on each film (~1x10^5 cells per glass cover slip). The protocol that initially took 6 weeks to produce 8 collagen film stacks, can now reproduce in 3 days, a stack of over 20 collagen films, populated by alternating fluorescently labeled colors (green and orange) of cells. The collagen films were thin and stacked in an efficient manner, and the corneal stromal fibroblasts were aligned in parallel on each collagen film as seen in figure 3.2. The alignment is thought to be due to the surface tension produced between the plastic of the Petri dish, the glass cover slips and thin collagen film. Thereby, stretching the collagen fibers along the glass cover slips in the direction the collagen was spread in the Petri dish before fibrillogenesis. Thus, when the cells are plated on top of the collagen films, they spread over a semi-organized collagen matrix that allows the cells to attach along the collagen fibrils and therefore align as shown in figure 3.3.

Day 3 of the protocol previously described entailed manually cutting each collagen film and stacking it on a collagen sponge base to provide nutrients to the cells during stacking. During the early stages of this protocol the collagen sheets had very poor

adhesion to each other, and as the collagen stack increased in size, it was challenging to keep the collagen films in place. This was exacerbated when culture media was added to supply the cells with nutrients since the media would tend to destabilize the stack and sometimes cause the layers to separate and float in the culture media. The alternate option was to reduce the amount of media to the collagen stack but this subsequently reduced the viability of the cells dramatically. As a result, fibronectin, which is an adhesive protein, was added in between the collagen films and acted as biological "glue" that kept the stack intact. Even though the collagen stack is supported on a collagen sponge with culture media, the cells were still poorly nourished during the 3 hour stacking process that occurs during day 3. As a consequence, once the stack is complete, it is sandwiched by another collagen sponge placed on top of the stack which is then completely immersed in media. In addition to supplying nutrition to the cells in the collagen film stack, the sponges are also somewhat compressing the collagen film stack, and in the process making it much thinner. This feature will be further discussed when considering the optical properties of this collagen film stack.

When pouring the collagen on day 1, the direction in which the collagen was "aligned" was noted on the Petri dish. Therefore the cell alignment on each collagen film was known so that when the films are being stacked, conscious effort was made to arrange each collagen film orthogonally to the adjacent collagen films. This was shown in figure 3.6 where the films carrying CTO (Cell Tracker® Orange) labeled cells were thicker, because the cells were sectioned laterally on the x-y plane, than the films

carrying CTG (Cell Tracker® Green) labeled cells, in which the cells were coming out of the x-y plane. This suggests that the collagen film stack methodology mentioned above is an efficient, reliable and reproducible protocol that mimics the cellular and structural lamellar arrangement and organization to that observed in the corneal stroma.

The success of this methodology was further examined by paraffin embedding and sectioning the 10 collagen film stack as previously described, and shown in figure 3.7. It is important to note that the sections were not deparaffinized before examination by confocal microscopy. The Cell Tracker® dyes are non-specific cytosolic labels and the deparaffinzation process would wash out the fluorescent dye. As a result, figure 3.7 depicts the analogous z-scan projection acquired by compiling the set of *in vivo* confocal images of the collagen film stack. When comparing this cross section to that of a human corneal stroma as shown in figure 3.8, the results show structural homology between the collagen film stack and the human corneal stroma. This provides further evidence for the success of the methodology developed to construct an *in vitro* model that will mimic the *in vivo* lamellar organization of collagen and thus direct cellular organization.

When designing an artificial corneal stroma construct it is important to study the expression of marker cytoskeletal proteins (α-SMA, MHC, MLC, and Vim). The expression of these proteins in the corneal stromal fibroblasts in the artificial corneal stroma construct should be similar to that seen in the human corneal stroma tissue. This was demonstrated in figures 3.9 through 3.20 (a) and (b) when corneal stromal fibroblasts seeded on thin collagen sheets as described above, were compared with corneal stromal

fibroblasts in the human corneal stroma tissue as seen in figures 3.8 (a) and (b). The morphologies of the corneal stromal fibroblasts in both, the collagen thin films and human corneal stroma tissue were also similar and showed the extended morphology that pertains to the quiescent nature of the corneal stromal fibroblasts in the corneal stroma tissue. The morphology is governed by the expression of the cytoskeletal proteins, and this is well demonstrated in figure 3.11 (a) and (b) of MHC, figure 3.14 (a) and (b) of MLC, figure 3.17 (a) and (b) of α-SMA, and figure 3.20 (a) and (b) of Vim in the corneal stromal fibroblasts seeded on thin collagen sheets. The fibers of these cytoskeletal proteins are extended and are very clearly evident in the fluorescent images of these cells. These results show that the cytoskeletal fibers are interacting with the fiber alignment of the thin collagen sheets, which further demonstrates that the collagen fibers on the thin collagen sheets are extended and stretched in a similar pattern to that seen in the ECM of the human corneal stroma. This is somewhat different from the morphology of the corneal stromal fibroblasts seeded on the glass cover slips, seen in figures 3.9 through 3.20 (c) and (d). The glass cover slips are artificial substrates and provide a harsh attachment substrate for the corneal stromal fibroblasts. Even though the expression of the cytoskeletal proteins does not vary on the glass cover slips, the appearance of visible extended fibers as seen on the corneal stromal fibroblasts seeded on the thin collagen sheets is not present. Therefore, the interaction of the cytoskeletal fibers with the collagen fibers is essential for the corneal stromal fibroblasts to adapt the desired morphology in the human corneal stroma tissue.

The main purpose of designing an artificial corneal stroma; that mimics the structural organization of components, cellular arrangement and protein expression of a human corneal stroma, is to produce a perfectly transparent living lens that can replace the human corneal stroma in the event that its function is impaired or damaged. The cornea is a perfect example of how structure dictates function of a tissue, which is why it is essential to study the optical properties of the corneal stroma construct. First, the percentage transmission of two 20 film collagen stacks were measured as mentioned above, and seen in figure 3.21. The first sample which was sandwiched between 2 collagen sponges gave a percentage transmission of 50%, and the second sample which was not sandwiched by collagen sponges gave a percentage transmission of 40% at 700nm. These numbers are comparable to the 57% transmission obtained by Orwin et al.[63] when they augment collagen sponges with chondriotin sulphate, and is much higher than the 34% transmission of collagen sponges alone[63] , and 5% transmission of collagen gels also at 700nm[63] . Despite the fact these values are far from the 98% transmission of the human cornea *in vivo*, it is important to note that the only way to reach complete optical transparency is if all the corneal components (stroma, epithelium, and endothelium) are in their optimal structural and cellular organization to prevent any light scattering. It is the collaborative "constructive interference" of all the corneal components that allow the cornea to act as a living lens, and any "destructive interference" will result in the increased opacity and compromised vision.

The higher percentage transmission obtained with the 20 film collagen stack that was sandwiched between two collagen sponges, was due to the fact that the sponges were "compressing" the stack thereby making it thinner. The sponges were absorbing some of the media, thereby bringing the extended collagen fibers closer to each other without compromising the viability of the corneal stromal fibroblasts seeded on top of each collagen film, or the exchange of the media throughout the collagen film stack. This state of hydration the collagen sponges provided the construct could be analogous to the function the epithelium and endothelium add to the corneal stroma in the cornea *in vivo*. The endothelium pumps the water into the corneal stroma, and the epithelium and tear film control evaporative losses. A limiting factor to the corneal collagen construct is that it does not have the stiffness to provide the curvature found in the human cornea, which is an important characteristic that makes the cornea a living lens, and contributes over 60% of the focusing power of the eye.

The transparency of the two samples were further investigated by placing them on typed text as described above and seen in figure 3.22. The collagen stacks indicated in figure 3.22 (a) and (c), were compressed by the collagen sponges, and showed more transparency and therefore visibility of the typed text than the uncompressed collagen stack indicated in figure 3.22 (b). The thicker sample was more opaque, further reinforcing the idea that the inter-lamellar distances between the collagen fibers is crucial for the transparency of the collagen film construct.

Finally, the optical activity of the collagen film construct was demonstrated by testing its polarization between two polarizers as described above. The results indicated in figures 3.23 and 3.24 that the collagen film construct was optically active. It was completely polarized when the second polarizer was at 0° and 180° (the polarizers are on the same principal axis), shown in figure 3.24 (a) and (f); and was completely depolarized when the second polarizer was at 90° (the second polarizer was perpendicular to the principal axis), shown in figure 3.24 (c).

The findings presented in this project provide strong evidence that the model developed is a successful representation of the human corneal stroma. These results included: designing a methodology to produce a collagen film stack, together with its structural and architectural integrity; a demonstration of the cytoskeletal protein expression and morphology of the corneal stromal fibroblasts in the collagen film stack; and an evaluation of its transparency and optical properties. ECM organization directs cellular organization in the corneal stroma. It is feasible to artificially construct a corneal stroma by stacking thin collagen sheets of collagen seeded with corneal stromal fibroblasts. The corneal stromal fibroblasts interact with the aligned collagen fibers in a fashion that resembles the structural architecture of the corneal stroma which is consequence to its transparency and optical properties.

CHAPTER V

FUTURE DIRECTIONS

This study concluded that collagen organization directs cellular organization in the corneal stromas, which then lead to examining the feasibility of constructing a model that will mimic the lamellar organization of collagen and thus direct cellular organization in the corneal stroma. The methodology that was designed utilized collagen type I to make thin films (~100μm) that provided an environment for corneal stromal fibroblasts to attach and align in the direction of the collagen fibers. This model was then examined for its cytoskeletal protein expression and optical properties in comparison to the human corneal stroma. One goal for future directions would involve testing the durability of the corneal stromal construct by adding more collagen films to the stack as well as enhancing the viability of the corneal stromal fibroblasts as the stack increases in size. Additional studies should focus on making the stack thinner but also avoiding its compaction to the extent of compromising the access of nutrients to the corneal stromal fibroblasts for their survival; this might include keeping the corneal stromal construct sandwiched between collagen sponges for longer periods of time, with more medium to circulate between and through the permeable thin collagen films and cells. The transparency experiments demonstrated that higher percentage transmissions are derived results from the thinner corneal stromal constructs. Thus having the stack sandwiched between collagen sponges for longer periods of time might make the corneal stromal construct function more

efficiently as a living lens. A long term direction would be to use this corneal stromal construct in clinical studies in the treatment of damaged corneal stromas.

Another aspect of this study would be to compare the collagen film stack with PMMA stacks. PMMA, as described earlier, is an FDA approved polymer used in the manufacture of contact lenses and intraocular lenses. It shows great promise for enhancing visual acuity in the eye due to its transparent characteristics. A comprehensive study comparing collagen and PMMA would entail molding PMMA into thin sheets of similar thickness as the collagen sheets produced through the methodology described in chapter III (~100μm). Corneal stromal fibroblast can then be seeded on the PMMA membrane sheets and stacked to resemble the structural organization of the corneal stroma. The collagen corneal stromal construct (stack) and the PMMA sheet stack could be compared in terms of feasibility, efficiency and reproducibility of assembling each type of model, furthermore, the long term survival of the corneal stromal fibroblasts on PMMA as opposed to collagen films should be examined, this could be a challenge since PMMA is impermeable and might prevent the transport of nutrient to the corneal stromal fibroblasts. An observation that was made while making the thin collagen films was that the surface tension between the plastic, glass cover slips and the collagen, allowed the collagen fibers to align and provide the environment for the corneal stromal fibroblasts to align in the direction of the collagen fibers. This could be another challenge for the PMMA model since the sheets are pre-assembled and the organization of the polymer's fibers can not be controlled unless the PMMA membranes are "machined" to create

surface topography similar to aligned collagen fibers. In addition, the hydrophobic nature of the PMMA membranes might prevent adhesion of the sheets to each other, which might be a problem when stacking the PMMA construct. Therefore future work might concentrate on combining PMMA and collagen to produce a heterogeneous stack that would have transparency, stiffness (PMMA), bio-stability, permeability and adhesive nature (collagen).

A lot of work in the field of tissue engineering is focused on electrospinning different polymers to generate nanofibers. This is pertinent for the stromal structure because of the inter-lamellar organization of the ECM and corneal stromal fibroblasts. Therefore, future work should address electrospinning collagen, or PMMA nanofibers coated with collagen control the alignment of the fibers and therefore cells. Pre-assembly of these into sheets would optimize the structural and mechanical properties of a corneal stromal stack. Another aspect of this study would be to use the methodology described in chapter III in other tissue engineering applications such as blood vessels and lung tissue.

The figures which follow are examples of exploring the possibilities discussed for future work. This work is being done in collaboration with D. Brian Hover (Advanced Optical; Alb. New Mexico) and Dr. Jeff Cotter (Department of Chemistry, Texas Christian University (TCU), Fort Worth Texas).

PRELIMINARY DATA FOR FUTURE DIRECTIONS

Figure 5.1 (a) and (b): preliminary data demonstrating a stack of 8 PMMA films seeded with corneal stromal fibroblasts labeled with Cell Tracker Orange® and Green® under confocal microscopy. The stack was placed in a 6-well plate and immersed in media, due to the non-adhesive nature of PMMA, the membranes dis-assembled from the stack; the sheets separated and could not be controlled. The thick green layer at the top of figure 5.1 (b) shows one of the PMMA membranes seeded with cells labeled with Cell Tracker Green® folded on itself. The membranes in figure 5.1 (a) are slanted, the distances between the sheets are irregular, and inconsistent with the orange and green alternations in labeled cells seeded on the PMMA during assembly.
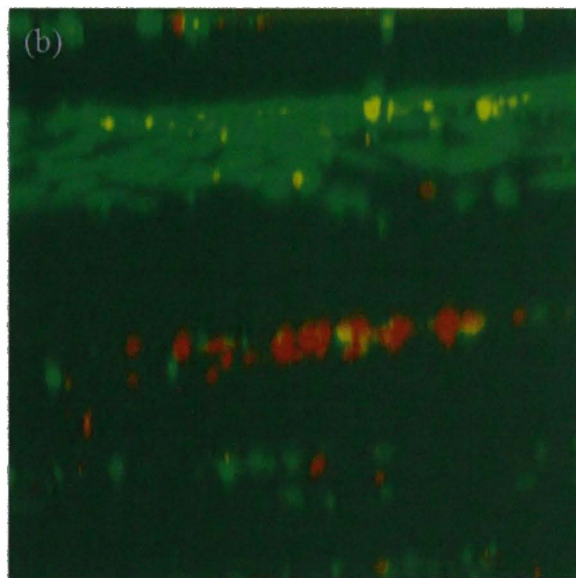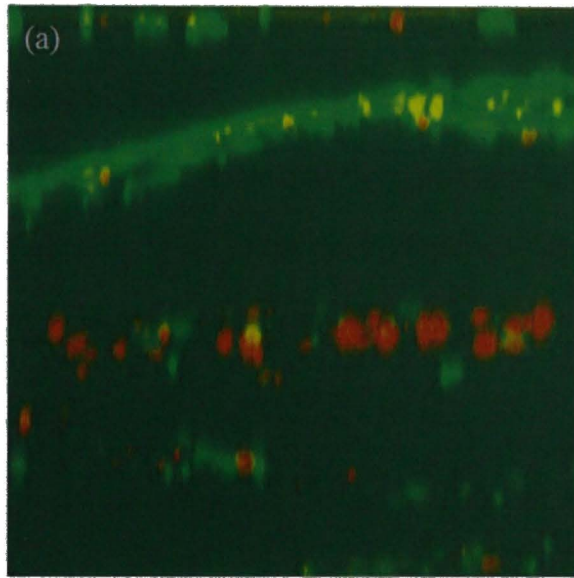
Figure 5.2: scanning electron microscope (SEM) images demonstrating preliminary data on electrospunn collagen at 1600x (a), 2000x (b), 3000x (c), and 4000x (d) magnification. Collagen type I solution traveled through a positively charged capillary tip to produce long micro and nano-fibers. Once the electrostatic forces between the tip and grounded target (aluminum surface) were larger then the surface tension of the collagen solution; the collagen fibers jet out of the capillary tip onto to the aluminum surface. Some of the fibers shown in figure 5.2 (b) and (c) are aligned in parallel and cross link in an orthogonal fashion.
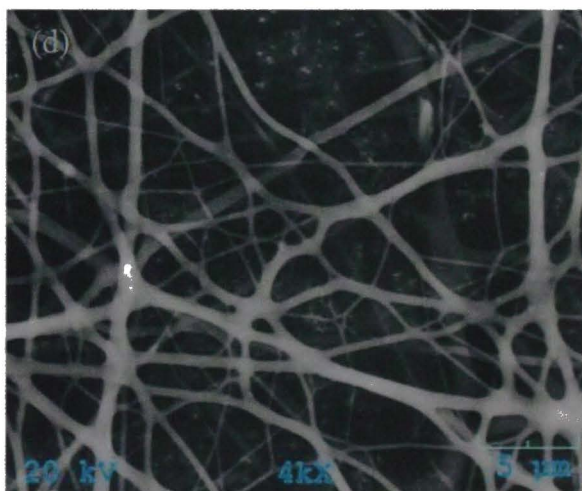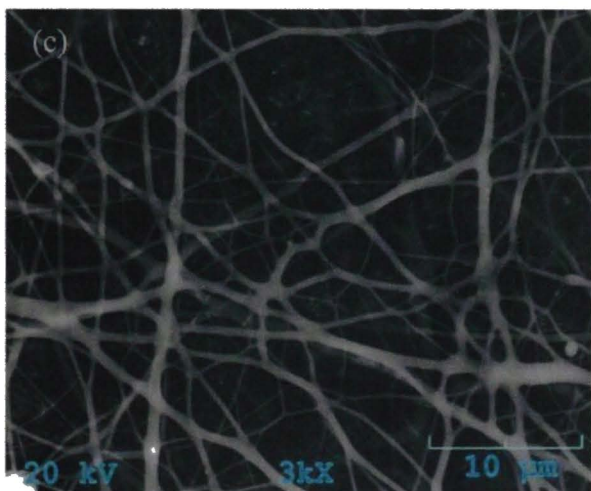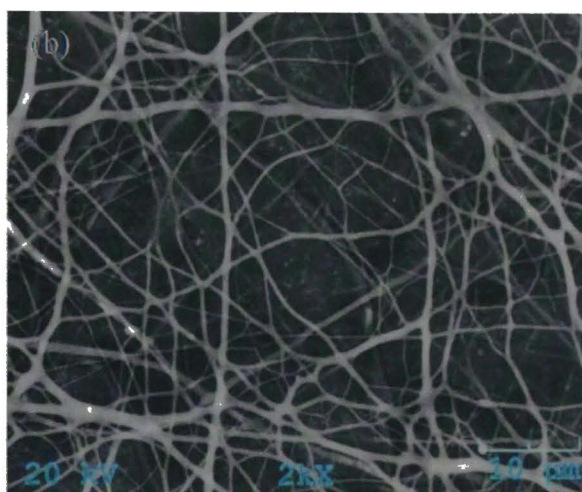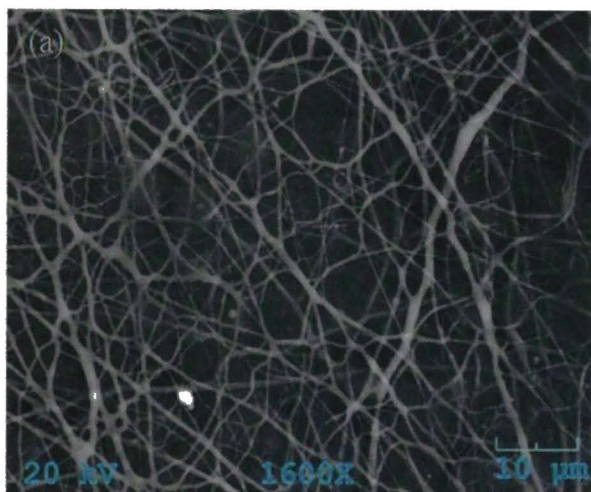
Figure 5.3: preliminary data demonstrating the alignment of corneal stromal fibroblasts on electrospunn collagen at 40x magnification under confocal microscope (a) and (c), and phase contrast (b) and (d). Electrospunn collagen was prepared by Dr. Jeff Cotter at TCU as described above. The collagen fibers were sterilized under UV, and cultured in 10% FBS in DMEM, corneal stromal fibroblasts transfected with GFP was seeded on top of the collagen fibers and allowed to attach overnight. The corneal stromal fibroblasts attached to the collagen fibers are aligned along the length of the fibers.

(c)

200 μm

(d)

200 μm
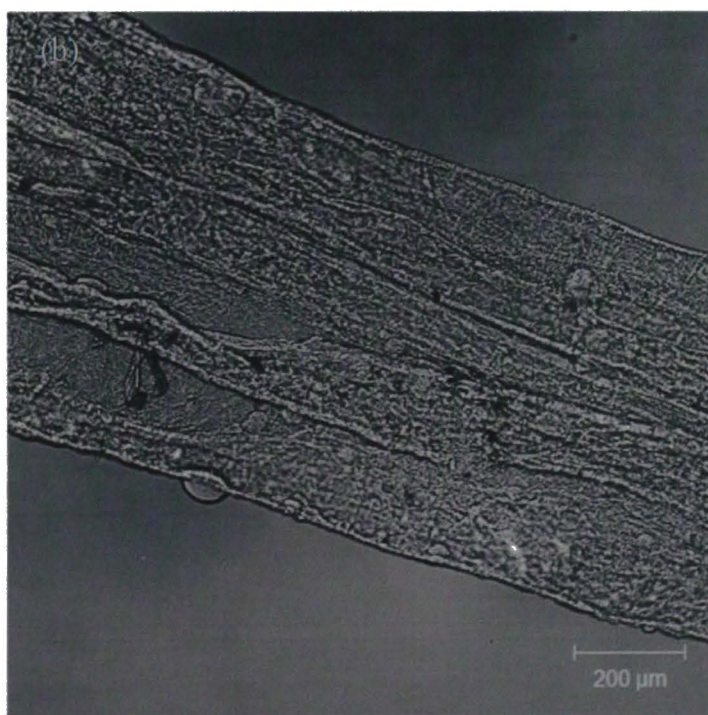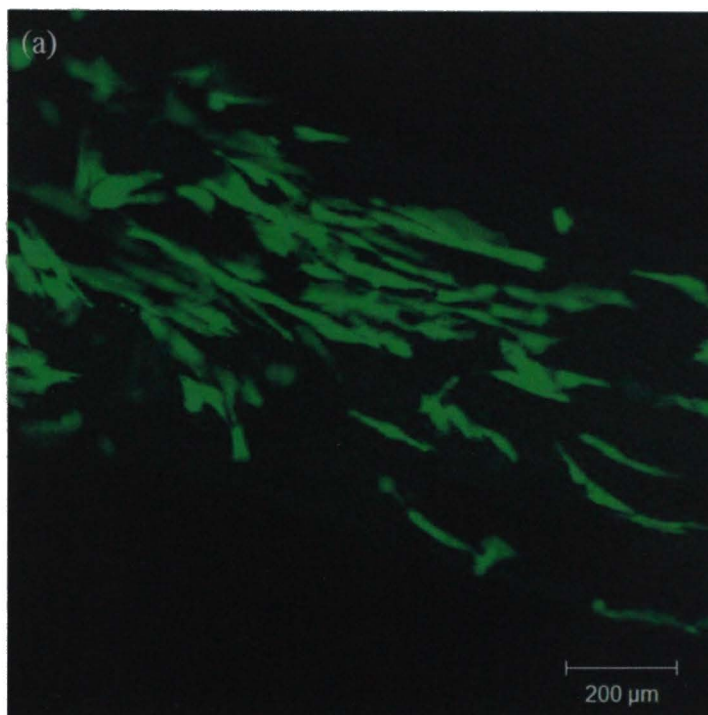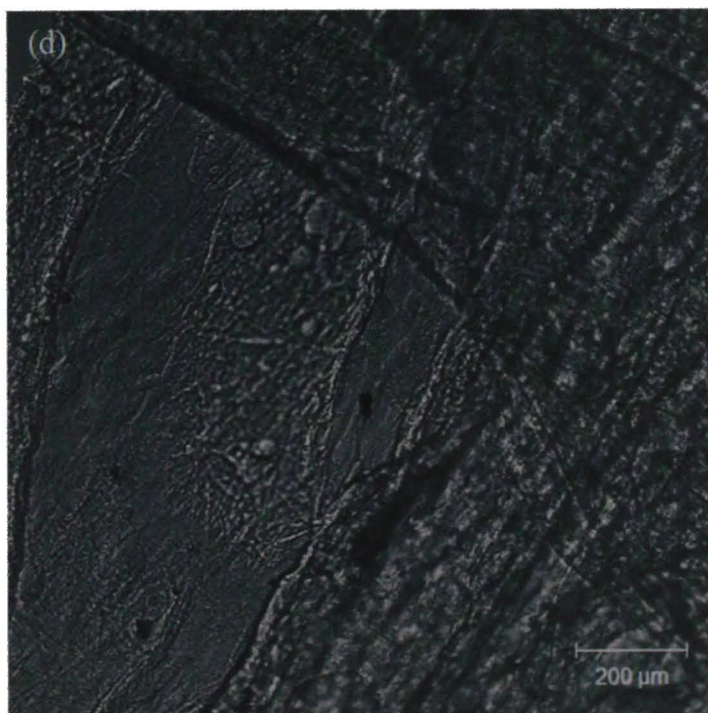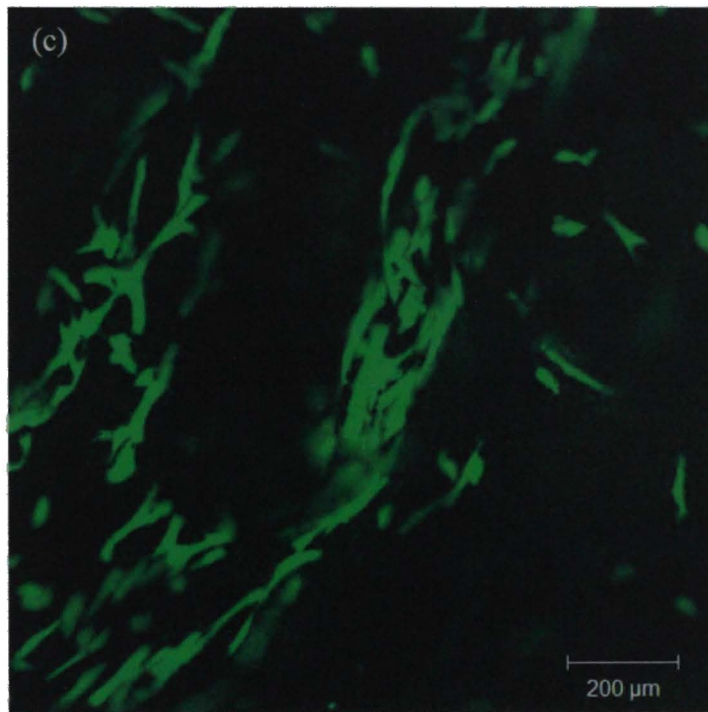
BIBLIOGRAPHY

1. Liliensiek SJ, Campbell S, Nealey PF, Murphy CJ. The scale of substratum topographic features modulates proliferation of corneal epithelial cells and corneal fibroblasts. J Biomed Mater Res A 2006; 79:185-192.

2. Taliana L. *The development of stratified corneal epithelium.* [PhD]. University of New South Wales; 1999.

3. Torbet J, Malbouyres M, Builles N, Justin V, Roulet M, Damour O, Oldberg A, Ruggiero F, Hulmes DJ. Orthogonal scaffold of magnetically aligned collagen lamellae for corneal stroma reconstruction. Biomaterials 2007; 28:4268-4276.

4. Dimitrijevich SD. Cornea and sclera. 2002.

5. Germain L, Carrier P, Auger FA, Salesse C, Guerin SL. Can we produce a human corneal equivalent by tissue engineering? Prog Retin Eye Res 2000; 19:497-527.

6. Ng CP, Swartz MA. Mechanisms of interstitial flow-induced remodeling of fibroblast-collagen cultures. Ann Biomed Eng 2006; 34:446-454.

7. Myllyharju J, Kivirikko KI. Collagens and collagen-related diseases. Ann Med 2001; 33:7-21.

8. Ruberti JW, Hallab NJ. Strain-controlled enzymatic cleavage of collagen in loaded matrix. Biochem Biophys Res Commun 2005; 336:483-489.

9. Garret RH, Grisham CM. *Biochemistry.* second edition ed. Saunders College Publishing; 1999.

10. mathews CK, Van Holde KE, Ahern K. G. *Biochemistry Third Edition.* 3rd edition ed. San Francisco, CA: Robin Heyden; 2000.

11. Harrington WF. *Collagen.* Vol 3. 1st ed. Johns Hopkins University: McCollum-Pratt Institute.

12. Carlsson DJ, Li F, Shimmura S, Griffith M. Bioengineered corneas: How close are we? Curr Opin Ophthalmol 2003; 14:192-197.

13. Hu X, Lui W, Cui L, Wang M, Cao Y. Tissue engineering of nearly transparent corneal stroma. Tissue Eng 2005; 11:1710-1717.

14. Crabb RA, Chau EP, Evans MC, Barocas VH, Hubel A. Biomechanical and microstructural characteristics of a collagen film-based corneal stroma equivalent. Tissue Eng 2006; 12:1565-1575.

15. Myung D, Koh W, Bakri A, Zhang F, Marshall A, Ko J, Noolandi J, Carrasco M, Cochran JR, Frank CW, Ta CN. Design and fabrication of an artificial cornea based on a

photolithographically patterned hydrogel construct. Biomed Microdevices 2007; 9:911-922.

16. Yiu SC, Thomas PB, Nguyen P. Ocular surface reconstruction: Recent advances and future outlook. Curr Opin Ophthalmol 2007; 18:509-514.

17. Schwab IR, Reyes M, Isseroff RR. Successful transplantation of bioengineered tissue replacements in patients with ocular surface disease. Cornea 2000; 19:421-426.

18. Hsiue GH, Lai JY, Chen KH, Hsu WM. A novel strategy for corneal endothelial reconstruction with a bioengineered cell sheet. Transplantation 2006; 81:473-476.

19. World Health Organization. Magnitude and causes of visual impairment. 2004; 282.

20. Hu CY, Tung HC. Managing keratoconus with reverse-geometry and dual-geometry contact lenses: A case report. Eye Contact Lens 2008; 34:71-75.

21. Rabinowitz YS. Keratoconus. Surv Ophthalmol 1998; 42:297-319.

22. Cristina Kenney M, Brown DJ. The cascade hypothesis of keratoconus. Cont Lens Anterior Eye 2003; 26:139-146.

23. Hollingsworth JG, Efron N, Tullo AB. In vivo corneal confocal microscopy in keratoconus. Ophthalmic Physiol Opt 2005; 25:254-260.

24. Petroll WM, Cavanagh HD, Barry P, Andrews P, Jester JV. Quantitative analysis of stress fiber orientation during corneal wound contraction. J Cell Sci 1993; 104 (Pt 2):353-363.

25. Pandrowala H, Bansal A, Vemuganti GK, Rao GN. Frequency, distribution, and outcome of keratoplasty for corneal dystrophies at a tertiary eye care center in south india. Cornea 2004; 23:541-546.

26. Ares C, Kasner OP. Bleb needle redirection for the treatment of early postoperative trabeculectomy leaks: A novel approach. Can J Ophthalmol 2008; 43:225-228.

27. Parks R. Trabeculectomy (filtration surgery) for glaucoma. 2006; 2008:1.

28. Fong CS. Refractive surgery: The future of perfect vision? Singapore Med J 2007; 48:709-18; quiz 719.

29. Myung D, Duhamel PE, Cochran JR, Noolandi J, Ta CN, Frank CW. Development of hydrogel-based keratoprostheses: A materials perspective. Biotechnol Prog 2008.

30. Khan B, Dudenhoefer EJ, Dohlman CH. Keratoprosthesis: An update. Curr Opin Ophthalmol 2001; 12:282-287.

31. Nouri M, Terada H, Alfonso EC, Foster CS, Durand ML, Dohlman CH. Endophthalmitis after keratoprosthesis: Incidence, bacterial causes, and risk factors. Arch Ophthalmol 2001; 119:484-489.

32. Hicks CR, Werner L, Vijayasekaran S, Mamalis N, Apple DJ. Histology of AlphaCor skirts: Evaluation of biointegration. Cornea 2005; 24:933-940.

33. Jacob JT, Rochefort JR, Bi J, Gebhardt BM. Corneal epithelial cell growth over tethered-protein/peptide surface-modified hydrogels. J Biomed Mater Res B Appl Biomater 2005; 72:198-205.

34. Uchino Y, Shimmura S, Miyashita H, Taguchi T, Kobayashi H, Shimazaki J, Tanaka J, Tsubota K. Amniotic membrane immobilized poly(vinyl alcohol) hybrid polymer as an artificial cornea scaffold that supports a stratified and differentiated corneal epithelium. J Biomed Mater Res B Appl Biomater 2007; 81:201-206.

35. Miyashita H, Shimmura S, Kobayashi H, Taguchi T, Asano-Kato N, Uchino Y, Kato M, Shimazaki J, Tanaka J, Tsubota K. Collagen-immobilized poly(vinyl alcohol) as an artificial cornea scaffold that supports a stratified corneal epithelium. J Biomed Mater Res B Appl Biomater 2006; 76:56-63.

36. Barnes CP, Sell SA, Boland ED, Simpson DG, Bowlin GL. Nanofiber technology: Designing the next generation of tissue engineering scaffolds. Adv Drug Deliv Rev 2007; 59:1413-1433.

37. Li D, McCann JT, Xia Y. Use of electrospinning to directly fabricate hollow nanofibers with functionalized inner and outer surfaces. Small 2005; 1:83-86.

38. Ma Z, Kotaki M, Inai R, Ramakrishna S. Potential of nanofiber matrix as tissue-engineering scaffolds. Tissue Eng 2005; 11:101-109.

39. Murugan R, Huang ZM, Yang F, Ramakrishna S. Nanofibrous scaffold engineering using electrospinning. J Nanosci Nanotechnol 2007; 7:4595-4603.

40. Griffith M, Hakim M, Shimmura S, Watsky MA, Li F, Carlsson D, Doillon CJ, Nakamura M, Suuronen E, Shinozaki N, Nakata K, Sheardown H. Artificial human corneas: Scaffolds for transplantation and host regeneration. Cornea 2002; 21:S54-61.

41. Borene ML, Barocas VH, Hubel A. Mechanical and cellular changes during compaction of a collagen-sponge-based corneal stromal equivalent. Ann Biomed Eng 2004; 32:274-283.

42. Doillon CJ, Watsky MA, Hakim M, Wang J, Munger R, Laycock N, Osborne R, Griffith M. A collagen-based scaffold for a tissue engineered human cornea: Physical and physiological properties. Int J Artif Organs 2003; 26:764-773.

43. Greiling TM, Clark JI. The transparent lens and cornea in the mouse and zebra fish eye. Semin Cell Dev Biol 2008; 19:94-99.

44. Meek KM, Leonard DW, Connon CJ, Dennis S, Khan S. Transparency, swelling and scarring in the corneal stroma. Eye 2003; 17:927-936.

45. Jayaraman K, Kotaki M, Zhang Y, Mo X, Ramakrishna S. Recent advances in polymer nanofibers. J Nanosci Nanotechnol 2004; 4:52-65.

46. Yang J, Yamato M, Kohno C, Nishimoto A, Sekine H, Fukai F, Okano T. Cell sheet engineering: Recreating tissues without biodegradable scaffolds. Biomaterials 2005; 26:6415-6422.

47. Yang J, Yamato M, Nishida K, Ohki T, Kanzaki M, Sekine H, Shimizu T, Okano T. Cell delivery in regenerative medicine: The cell sheet engineering approach. J Control Release 2006; 116:193-203.

48. Vrana NE, Elsheikh A, Builles N, Damour O, Hasirci V. Effect of human corneal keratocytes and retinal pigment epithelial cells on the mechanical properties of micropatterned collagen films. Biomaterials 2007; 28:4303-4310.

49. Dimitrijevich SD. Troubleshooting connective tissue equivilants.

50. Dimitrijevich SD, Gracy RW. Non-contracting tissue equivalents (skin, cornea and conjunctiva). 2002.

51. Dimitrijevich SD, Reese TJ, Gracy, R.W.:, Oakford, L.X., Howe WE. A transmission electron microscopic study of methods for harvesting epithelial cells from human corneal tissue. Proc 49th An Meeting of Electron Microscopy Soc Amer 1991.

52. Dimitrijevich, S.D., Reese, T.J., Yorio, T., and Gracy, R.W. In vitro models of human ocular tissue: Part I. corneal epithelium equivalent. Invest Ophthalmol Vis Sci 1995; 36:S701.

53. Dimitrijevich, S.D., Reese, T.J., Yorio, T., and Gracy, R.W. In vitro model of the human corneal endothelium. Invest Ophthalmol Vis Sci 1994; 35:1602.

54. Shankardas J. *In vitro studies in tissue contraction and scar formation.* ; 2004.

55. Barhoumi R, Bowen JA, Stein LS, Echols J, Burghardt RC. Concurrent analysis of intracellular glutathione content and gap junctional intercellular communication. Cytometry 1993; 14:747-756.

56. Molecular Probes, Invitrogen Detection Technologies. Cell tracker probes for long-term tracing of living cells. 2008; 2008:5.

57. Poot M, Kavanagh TJ, Kang HC, Haugland RP, Rabinovitch PS. Flow cytometric analysis of cell cycle-dependent changes in cell thiol level by combining a new laser dye with hoechst 33342. Cytometry 1991; 12:184-187.

58. Meyer-ter-Vehn T, Sieprath S, Katzenberger B, Gebhardt S, Grehn F, Schlunck G. Contractility as a prerequisite for TGF-beta-induced myofibroblast transdifferentiation in human tenon fibroblasts. Invest Ophthalmol Vis Sci 2006; 47:4895-4904.

59. Rice NA, Leinwand LA. Skeletal myosin heavy chain function in cultured lung myofibroblasts. J Cell Biol 2003; 163:119-129.

60. Lister I, Roberts R, Schmitz S, Walker M, Trinick J, Veigel C, Buss F, Kendrick-Jones J. Myosin VI: A multifunctional motor. Biochem Soc Trans 2004; 32:685-688.

61. Komatsu S, Ikebe M. The phosphorylation of myosin II at the Ser1 and Ser2 is critical for normal platelet-derived growth factor induced reorganization of myosin filaments. Mol Biol Cell 2007; 18:5081-5090.

62. Cooper GM. *The Cell: A Molecular Approach.* Dana-Farber Cancer Institute, Harvard Medical School, MA: ASM Press, Sinauer Associates, Inc.; 1997.

63. Orwin EJ, Lee S, Raub C, Icenogle T, Arman M, Cho A, Lovec R, Malone A, Haskell RC, Hoeling BM, Petersen DC. Optical coherence microscopy for the evaluation of a tissue-engineered artificial cornea. Conf Proc IEEE Eng Med Biol Soc 2004; 2:1218-1221.

64. Lacowitz JR. *Principles of Fluorescence Spectroscopy.* 3rd ed. University of Maryland School of Medicine, Baltimore, Maryland: Springer; 2006.